Norwegian University
of Life Sciences

Master's Thesis 2019 30 ECTS
Faculty of Science and Technology

Aerodynamic Wind Analysis of Bridge Girder with CFD Calculations

Anne Marte Gaarder
Mechanics and Process Technology

Acknowledgement

This thesis is conducted as the final assessment on my master's degree in Mechanics and Process Technology at the Norwegian University of Life Science (NMBU), with specialisation in energy and process techniques. The main focus in this thesis is bridge girders and aerodynamics and there were conducted much ground work to get the knowledge for this theme and the understanding on how wind and bridge girders work together. There are looked at compliance between one bridge girder from IFE in relation to previous work and simulations. During my time as a student I have gotten both friends and professional experience that will guide me through life.

I am grateful to my supervisor Tor Anders Nygaard at NMBU for the introduction, guidance and help with my thesis, and my assistant supervisor Luca Oggiano at the Institute for Energy Technology for the assistance with all my simulations and analyses.
I also am grateful to my friends and family for the support over these last few months, I could not have done this without your support and motivation. Thanks to my fellow students for laughter and inspiration during this period, and for lots of fun over the last years.

Anne Marte Gaarder

Ås, 14th of May 2019

Abstract

This thesis is a validation study of different bridge girder geometries. The initiative for the thesis is that today one must cross most of the fjords on the west coast of Norway by ferry. There are several projects studying the process of converting these ferry routes to bridges and in 2017 the Norwegian Public Road Administration published a report discussing the respective distances. The thesis is conducted in collaboration with the Institute of Energy Technology (IFE) and the bridge girder was considered and analysed when Hardangerbrua were built in 2013.

In the thesis there are conducted Computational Fluid Dynamic (CFD) simulations in the Computational Aided Engineering (CAE) program STAR CCM+. The bridge girder is analysed with different dimensions, angles of attack and velocities. It is discussed how these factors effects the lift, drag and pressure. After simulations on six different angles of attack, it shows that the lift and drag forces is changed in correlation with the angles of attack because of changes in pressure.

The simulations conducted in this thesis are compared to previous work on bridge girders. The bridge girders pressure is analysed with 3.0 m/s inlet velocity. While the bridge girder with different angles of attack from -10 degrees to 3 degrees are analysed with inlet velocity 8.0 m/s. The analyses shows that the simulations conducted in thesis has a good correlation with previous work and these bridge girder designs are valid in relation to previous analyses.

Sammendrag

Denne oppgaven ser på to ulike geometrier for brokasser. Bakgrunnen for oppgaven er at man i dag må krysse de fleste av fjordene på vestkysten av Norge med ferge. Det er flere prosjekter som omhandler dette og i 2017 ga Statens Vegvesen ut en rapport som omhandler de aktuelle strekningene. Oppgaven er skrevet i samarbeid med Institutt for Energiteknikk (IFE) og brokassen ble analysert i forbindelse med byggingen av Hardangerbrua før den sto ferdig i 2013.

Det har blitt gjennomført numeriske fluiddynamikk simulering i dataprogrammet STAR CCM+. Brokassen analysert i to dimensjoner og er det gjennomført simuleringer på vind med ulike innfallsvinkler og hvilken påvirkning vinklene har er diskutert i forhold til løft og drag. Etter at 6 ulike innfallsvinkler er analysert kommer det frem at løft og drag endrer seg med innfallsvinkelen på grunn av endringer i trykket.

Simuleringene som er gjennomført i denne oppgaven er sammenlignet med tidligere analyser av lignende brokasser. På den ene brokassen er det brukt en innløpshastighet på 3.0 m/s, mens den andre brokassen er analysert med innløpshastighet på 8.0 m/s og innfallsvinkler fra -10 til 3 grader. Analysene som er gjennomført viser at simuleringene som er gjennomført i denne oppgaven er valide i forhold til tidligere undersøkelser.

Table of Content

List of figures

List of tables

List of symbols

Symbol	Description	Unit
A	Area	m^2
U	Mean wind velocity	m/s
l	Length	m
ρ	Density	Kg/m^3
p	Pressure	Pa
μ	Dynamic viscosity	$Pa*s$
Re	Reynolds number	-
x, y, z	Cartesian structural global axis	-
υ	Kinematic viscosity	m^2/s
u^*	Friction velocity	m/s
α	Angle of attack	
Y	Specific weight	
y^+	Wall distance	-

List of abbreviations

CFD	Computational Fluid Dynamic
CAE	Computational Aided Engineering
CAD	Computer Aided Design
FSI	Fluid Structure Interaction
FEM	Finite Element Method
FEA	Finite Element Analysis
FVM	Finite Volume Method
VIV	Vortex Induced Vibrations
IFE	Institute for Energy Technology
NMBU	Norwegian University of Life Science
NTNU	Norwegian University of Science and Technology
E39	Europavei 39
SVV	Norwegian Public Road Administration
RANS	Reynolds-averaged Navier-Stokes equation
RMS	Roof mean square
GF	Growth Factor

1. Introduction

1.1. Background for the thesis

The background for this thesis is a collaboration with Institute for Energy Technology (IFE) and their wish to conduct a validation study of a bridge girder in comparison to other bridge girders already analysed.

The initiative for this thesis is that today one must cross most of the fjords in Western Norway by ferry and there are several large projects working on the project of converting parts of these ferry routs to tunnels or bridges. In the Norwegian Public Roads Administrations (SVV) rapport "Ferjefri E39" (*Ferjefri E39*, 2017) some of these routes are displayed and discussed. By changing from ferries to bridges the total travelling time between Kristiansand and Trondheim will be halved.

The focus on bridge girders is huge, and there are many thought on how to best design a bridge girder. The bridge girders used in this thesis are the same version of a bridge girder, but different dimensions are used in different parts of the analysis. The bridge girder took part in the development process of Hardangerbrua.

Figure 1.1 displays a 2D sketch of the general bridge girder model while Figure 1.2 shows the sketch in 3D. The traveling direction on the bridge girder in Figure 1.2 is in z-direction.

It is given that the reader has aerodynamic and physics insight at university level before reading this thesis.

Since the aim for this thesis is simulation and not modelling, there will not be much focus on the modelling details in STAR CCM+.

Figure 1.1: Example on bridge girder from STAR CCM+. This design will be further discussed later in this thesis.

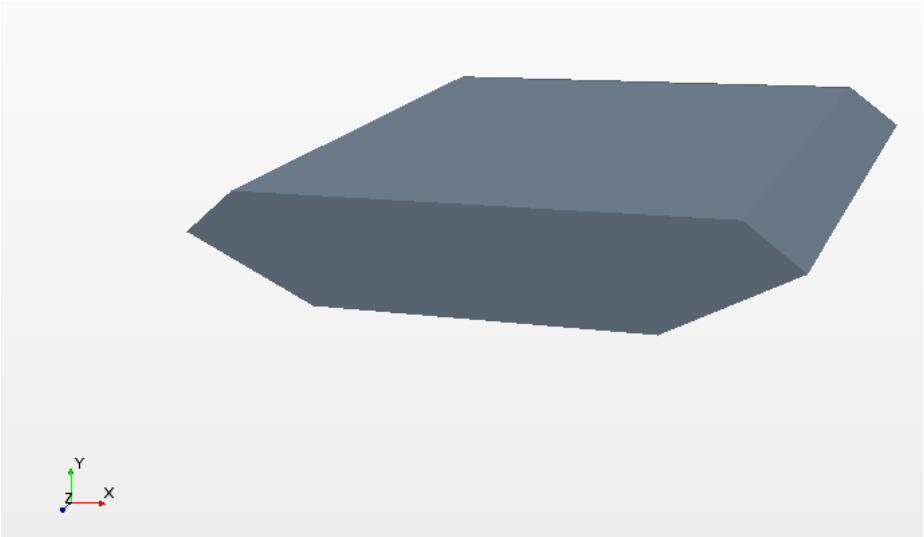

Figure 1.2: Bridge girder 3D-model from STAR CCM+.

1.2.Goal and objective

The goal for this thesis is to conduct a validation study of a bridge girders with grounds in the Hardangerbrua project. Different wind angles of attacks will be analysed, and pressure and velocity simulations will be conducted. All the analyses will be compared to previous work to see if the bridge girders meet the requirements relative to the wind flow. There will only be conducted 2D simulations and the bridge girders will be called alternative 1 and 2. Bridge girder alternative 1 will be analysed regarding pressure, while bridge girder alternative 2 will be simulated with different angles of attack and analysed regarding lift and drag behaviour.

1.3.Limitations

The scope for the project is defined by the following limitations:

- Only numerical analyses will be performed
- The geometry is supplied by IFE and the project group on Hardangerbrua so there will not be made any changes on this.
- Lack of bridge girder knowledge

1.4.Structure

Chapter 2 presents the theory used in this thesis. There will be theory on CFD-analysis, bridge constructions and wind forces.

Chapter 3 presents the methods used in this thesis. There is conducted a literature study that is presented in this chapter. How the results for this thesis is retrieved is also presented in this chapter.

Chapter 4 presents the simulations completed in STAR CCM+ for two different bridge girder dimensions and velocities in addition to analysis of rectangle and square 2D models. There will be velocity and pressure simulations for the perpendicular wind on bridge girder alternative 1. Then there will be simulations for different angles of attack for the bridge girder alternative 2.

Chapter 5 presents the results after conducting the simulations in STAR CCM+. There will first be conducted a pressure analysis for the square, rectangle and the bridge girder alternative 1, then there will be a lift and drag analysis for the bridge girder alternative 2.

Chapter 6 presents the discussion and the validation study of the conducted simulations and results. There are first presented a general discussion on bridge girders and simulations, and then the discussion for the square, rectangle and both bridge girders are presented.

Chapter 7 presents the conclusion and recommendations for further work.

2. Theory

2.1.CFD – analysis

Computational Fluid Dynamics (CFD) analysis or numerical fluid dynamic is a branch of fluid dynamics that uses numerical analysis and data structures to analyse and solve problems that involve fluid flow (Jayakumar et al., 2010).

In this thesis the simulations will be conducted in a computer aided program called STAR CCM+. The geometry is imported from a CAD file. To get more practical results some of the models are placed in a wind tunnel and real wind conditions are applied. Some of the comparable data in this thesis are analysed in a wind tunnel. By comparing the results from the wind tunnel and STAR CCM+ there are ground to see the validity of the STAR CCM+ simulations. If there is high consistence between the results STAR CCM+ can be used in the rest of the simulations. Even though the wind tunnel simulations are more accurate the STAR CCM+ simulations are cheaper and demands less resources than the wind tunnel simulations.

In CFD a grid system needs to fulfil two important criterions to be an accurate an optimum grid system. Firstly, the grid or cell height (y) away from the body should be at the viscous sublayer (for non-slip boundary condition) for an accurate modelling of the boundary layer flow, is known as near-wall treatment (Franke et al., 2011). In bridge and bluff body aerodynamics fields also, grids are generated by following this criterion (Bruno et al., 2010). In viscous sublayers, the viscous stress dominants over the Reynolds stress and situate where the non-dimensional wall distance (y^+) is less than a value of 5 (Pope & Pope, 2000) as show in Figure 2.1, the y^+ value can be defined as,

$$y^+ = \frac{u^* * y}{v}$$

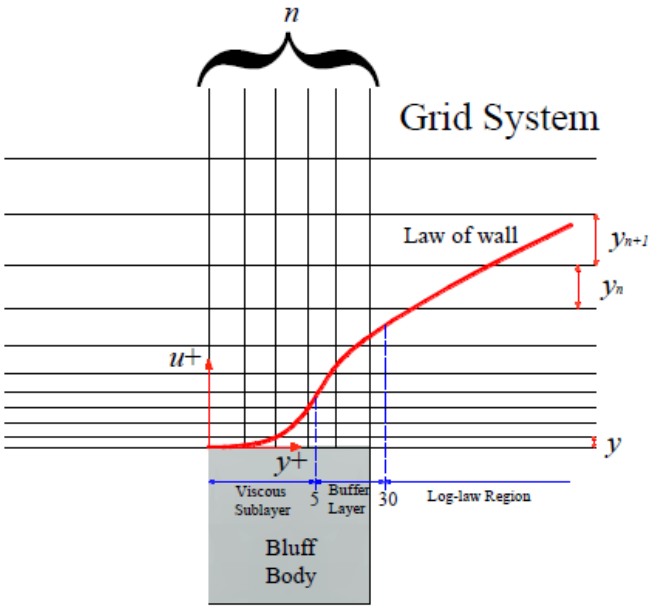

Figure 2.1: Concept of near-wall treatment and various important notations in grid system (Haque, 2015).

2.1.1. Finite Element Method (FEM) and Finite Element Analysis (FEA)

FEM is a numerical method to solve problems connected to mathematical physics. Some typical areas of use are structural analysis, heat transfer, fluid flow, mass transfer and electromagnetic potential (Sjødin, 2016). Analysis of FEM is called Finite Element Analysis (FEA). An important advantage with FEM is its natural ability to handle deforming spatial domain, making it suitable for multi-physics simulations such as Fluid-structure interactions (FSI) (Helgedagsrud et al., 2018).

2.2.Bridge Girder

A bridge girder is the core of a bridge. The dimensioning of the bridge girder is essential in the design process of a bridge. The wind flow and other forces the bridge is exposed to must be considered when designing the bridge girder. Figure 2.2 shows bridge girders in a bridge assembly prosess.

Figure 2.2: Illustration of bridge girder being connected. The picture is found in (Haque, 2015)and (Science, 2013)

2.3.Hardangerbrua

Hardangerbrua is a bridge over Eidfjorden that is an arm from Hardangerfjorden. The bridge is part of the main road between Bergen and Oslo. It is a two-lane suspension bridge with a sidewalk for biking and walking. The bridge is the longest suspension bridge in Norway with its main holding of 1310 meter and a total length of 1380 meters. The bridge towers is 200 meters high and the sailing height is 55 meters (Ferde, 2019). The bridge is assembled by bridge girders, that each are 60 meters long.

The bridge was planned by SVV and visualized by Multiconsult.

2.4. Wind Forces

In the process of dimensioning a large bridge construction, wind is one of the biggest challenges. There are two different types of wind forces; static and dynamic. Static wind forces are calculated from the mean wind and dynamic wind forces due to vortex shedding, turbulence and motion induced load effect.

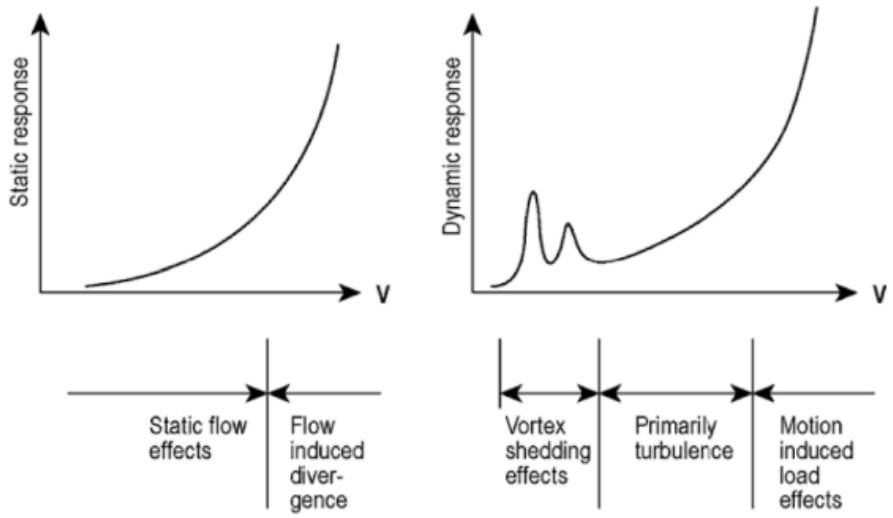

Figure 2.3:Strømmen (2010) displays the static and dynamic forces like this Typical response behaviour of slender civil engineering structures. I: (Strømmen, 2010) Theory of Bridge Aerodynamics, s. 2. Berlin: Springer Media.

Boundary Conditions

Boundary conditions are required to be defined for the boundaries of the computational domains and they appear as source terms. Various types of boundary conditions are implemented in bluff body aerodynamics field. Numerical result is highly influenced by the dimension of the flow domain and type of boundary condition. In case of 3D domain, four main parameters are: the upstream distance (distance between the inlet and object, X_u), the downstream distance (distance between the object and the outlet, X_d), height of the domain (H) and width of the domain (B) (Haque et al., 2013).

The boundary conditions used in this thesis are:

- Reference pressure, 0 Pa
- Inlet velocity, u, of 3.0 m/s and 8.0 m/s
- The air density, ρ, of 1.15 kg/m^3

Roughness

Surface roughness is expressed as the irregularities of material resulted from various machining operations. In quantifying surface roughness, average surface roughness definition, which is often represented with Ra symbol, is commonly used (Öktem et al., 2005).

2.4.1. Mean Wind

The statistical properties of the mean wind velocity U*(z)* are required in order to establish a basis for the calculations of structural design load effects during the weather conditions that have been deemed representative for the purpose of obtaining sufficient safety against structural failure.

Mean wind statistics must be based on data covering numerous meteorological observations over several years, as it is the values of U*(z)* under a large variation of weather conditions that are of interest. Such statistics are usually performed on the mean wind velocity at z = 10 m and averaged over a period of T = 10 min (Strømmen, 2010).

2.4.2. Static Wind Forces

The static wind forces are calculated from the mean wind and the resulting dynamic pressure and shear stresses that act on the bridge. The forces are called drag force, lift force and torque. The static forces are illustrated in Figure 2.4

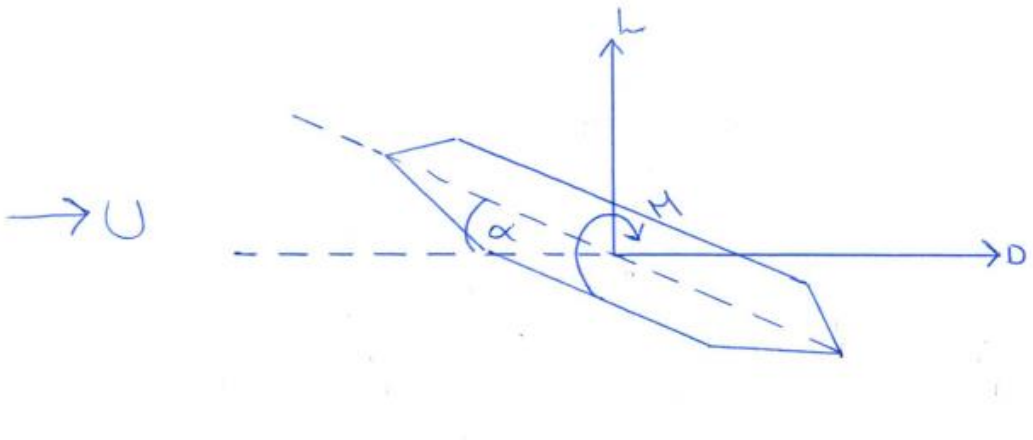

Figure 2.4: Static forces displayed together with angle of attack.

Angle of attack (α)

The angle of attack is the angle between the relative inlet wind and the actual inlet wind direction. In Figure 2.5 the angle of attack α is defined as the angle between the direction of flow and the unit normal joining x_{cp} and x_{cm}.

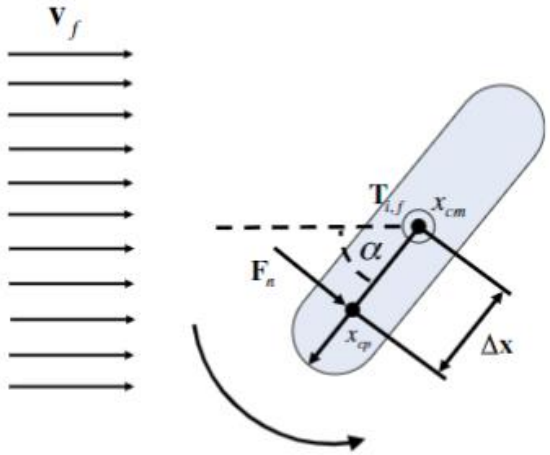

Figure 2.5: A spherocylinder subject to torque. The difference between the centre of pressure x_{cp} and the centre of mass x_{cm} leads to the development of an aerodynamic torque T_{if}. Δx is the distance between x_{cp} and x_{cm} (Mema et al., 2019).

Drag force (F_D)

When an object moves though a fluid as air or water the fluid exerts a drag force or retarding force that opposes the motion of the object (Tipler & Mosca, 2007). Lift and drag are displayed in Figure 2.4 and Figure 2.6.

Lift force (F_L)

For non-spherical particles suspended in a fluid flow, a shape induced lift force, similar to the concept of an aerofoil in aerodynamics, can significantly affect the trajectory of a particle. When the axis of an elongated particle, such as a spherocylindrical particle in this study, is inclined to the direction of relative fluid flow, the flow fields on the upper and lower sides of the particle differ. The pressure drops in regions of rapid flow while the pressure increases in regions where the fluid velocity decreases, thus leading to an asymmetric pressure distribution and inducing a lift force perpendicular to the direction of relative fluid flow (Mema et al., 2019).

Torque (F_T)

As demonstrated in the preceding sections, drag force acts in the direction of relative fluid flow and depends on particle orientation relative to the flow while lift force leads to a force perpendicular to the relative fluid flow. When the centre of pressure x_{cp} acting on a non-spherical particle does not coincide with the centre of mass of the particle x_{cm}, an aerodynamic pitching torque results and acts around the axis perpendicular to the plane of relative fluid velocity v'_{fi} and particle orientation vector u_i. The torque can change the angle of attack α of the particle (Mema et al., 2019).

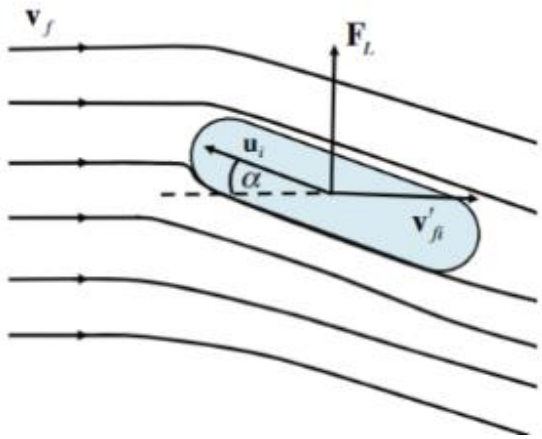

Figure 2.6: Lift vector orientation based on the relative velocity of the fluid with respect to the particle $v'_{fi} = v_f - v_i$ and particle orientation vector u_i. The angle of attack of the fluid flow α is also indicated on the figure (Mema et al., 2019).

Table 2.1: Equations for drag, lift and momentum. The equations are retrieved from Strømmen (2010).

	COEFFISIENT	
DRAG	$C_D = \frac{F_D}{qH}$	*Eq 2-1*
LIFT	$C_L = \frac{F_L}{qL}$	*Eq 2-2*
TORQUE	$C_M = \frac{F_T}{qL^2}$	*Eq 2-3*
BERNOULLI'S EQUATION	$q = \frac{1}{2}\rho u^2$	*Eq 2-4*

Where

- *ρ is air density*
- *u is the mean wind velocity*
- *H is height of bridge girder*
- *L is width of bridge girder*
- *q is the wind velocity pressure (Strømmen, 2010)*

Bernoulli's equation

Conservation of energy is governed by Bernoulli's equation. This equation relates three types of energy in a flow: pressure head, potential energy and kinetic energy. Several assumptions are made when considering Bernoulli's equation:

- Ideal flow, so viscosity is neglected
- Flow is steady state
- The equation is only valid along streamlines, not across
- Fluid is incompressible
- No energy is added or removed along a streamline.

The energy is often reported on a per unit weight basis, as in the following equation:

$$\frac{p}{\gamma} + z + \frac{u^2}{2g} = constant\ along\ streamline$$

Here, p denotes the pressure, γ is the specific weight of the fluid, z is the elevation, u the flow velocity and g is the gravity constant. An illustration of the Bernoulli principle is given in Figure 2.7, where the sum of pressure, potential and kinetic energy is the same at points 1 and 2 which lie on the same streamline. Bernoulli's equation can be expanded to include head losses for viscous flow

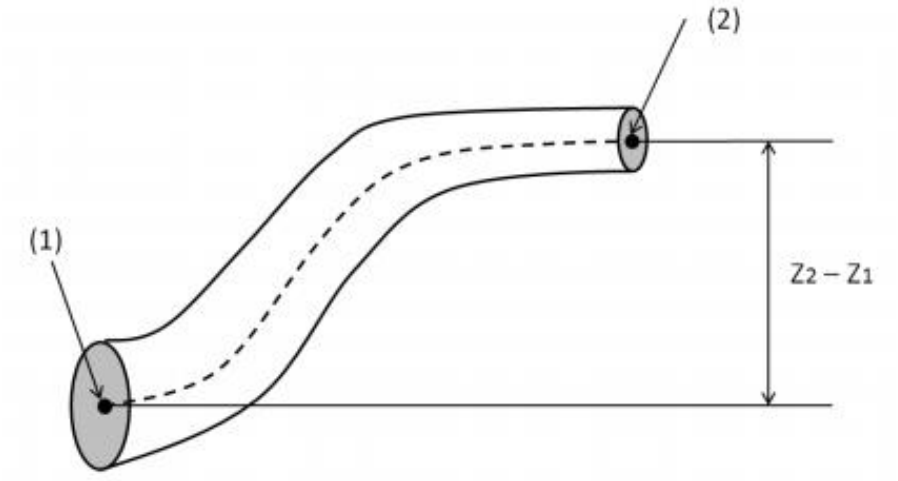

Figure 2.7: Sectioned pipe with streamline illustrating Bernoulli's principle (Weisstein, 2007).

Navier-Stokes

The general solution to flow problems is governed by the Navier-Stokes equations. They include both surface and body forces that act on the fluid, such as friction, gravity and pressure forces. The equations state that the sum of body and surface forces are equal to the change of momentum in the flow. The full Navier-Stokes equations form the basis of computational fluid dynamics (CFD).

$$-\frac{\partial p}{\partial x}+\mu\left(\frac{\partial^2 u}{\partial x^2}+\frac{\partial^2 u}{\partial y^2}+\frac{\partial^2 u}{\partial z^2}\right)=\rho\left(\frac{\partial u}{\partial t}+u\frac{\partial u}{\partial x}+v\frac{\partial u}{\partial y}+w\frac{\partial u}{\partial z}\right)$$

$$-\frac{\partial p}{\partial y}+\mu\left(\frac{\partial^2 v}{\partial x^2}+\frac{\partial^2 v}{\partial y^2}+\frac{\partial^2 v}{\partial z^2}\right)=\rho\left(\frac{\partial v}{\partial t}+u\frac{\partial v}{\partial x}+v\frac{\partial v}{\partial y}+w\frac{\partial v}{\partial z}\right)$$

$$-\rho g-\frac{\partial p}{\partial x}+\mu\left(\frac{\partial^2 w}{\partial x^2}+\frac{\partial^2 w}{\partial y^2}+\frac{\partial^2 w}{\partial z^2}\right)=\rho\left(\frac{\partial w}{\partial t}+u\frac{\partial w}{\partial x}+v\frac{\partial w}{\partial y}+w\frac{\partial w}{\partial z}\right)$$

On the left side of the equation the term ρg denotes the gravity force, the ∂p terms the pressure forces and the μ terms the frictional forces. The right side expresses the rate of change of momentum.

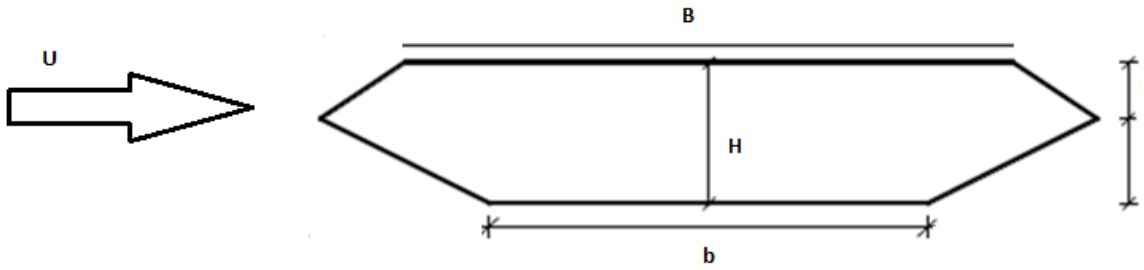

Figure 2.8: Bridge Girder sketch with wind directions.

Figure 2.8 presents the inlet wind direction (U) towards the bridge girder, in addition the dimensions (B, b and H) on the bridge girders are shown.

Width ratio (W)

The width ratio (W) is the relation between the bottom width (b) and top width of the bridge girder (B) (Yang et al., 2016). The aerodynamic response is dependent on the width ratio (Haque, 2015).

2.4.3. Dynamic wind forces

According to Strømmen (2010) there are four types of structural behaviour for a bridge section. First, there is the possibility of a static type of unstable behaviour in torsion, called static divergence. Second, there is the possibility of a dynamic type of unstable behaviour in the across wind vertical (z) direction, called galloping. Third, there is a possible unstable type of dynamic response in pure torsion, and finally, there is the possibility of an unstable type of dynamic response in combined motion of vertical displacement and torsion, called flutter.

Vortex Shedding

Vortex shedding is an oscillating flow that takes place when a fluid flows past a body at certain velocities, depending on the size and shape of the body (Wong & Chen, 1986). In Figure 2.3 the effects of vortex shedding are displayed.

Turbulence

Turbulence is changes in the wind over a short period of time.

2.5. Boundary Layer

The boundary layer is the area where the flow is close to the surface of the material it is passing. The velocity of the flow drops because of the friction between the flow and surface.

2.5.1. Reynolds number

Reynolds number describes the connection between a liquid or gas density and flow rate. When wind passes the bridge girder the flow rate gets separated. This separation is, especially for cross sections with rounded corners, dependant of Reynolds number, Re.

$$Re = \frac{UH}{\upsilon} \qquad \textit{Eq 2-5: Reynolds number}$$

Where U is the wind velocity, H is the bridge girders cross section height or width and the winds kinetic viscosity is $\upsilon = 1.529 * 10^{-5} m^2/s$ *(Montgomery, 1947).*

2.5.2. Laminar and turbulent flow

Laminar flow is flow based on small Reynolds number, Re, while turbulent flow is flow with higher Re. Re < 2000 gives a laminar flow, while Re > 2000 gives a turbulent flow (Kenis et al., 1999). Laminar flow is illustrated in Figure 2.9, while Figure 2.10 illustrates turbulent flow.

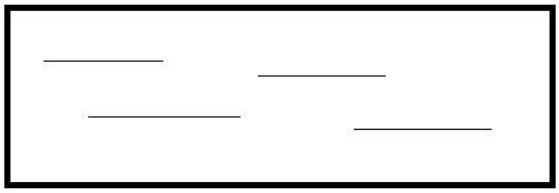

Figure 2.9: Sketch of laminar flow.

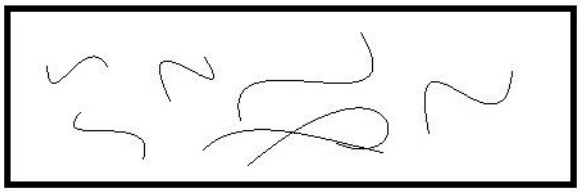

Figure 2.10: Sketch of turbulent flow.

2.5.3. K-Omega turbulence model

The k-omega turbulence model solves one equation for the turbulent kinetic energy k and a second equation for the specific turbulent dissipation rate (or turbulence frequency) ω (Menter, 1992).

2.6. Validation study

A validation study is conducted to compare the bridge girder design for the general bridge girder and earlier design models that is proven to be functional. The results from the simulations are crucial for the further work of the bridge girder on the general bridge girder, and to see if this bridge girder is valid compared to projects already conducted.

A validation is a process through which it is assessed how closely or accurately the numerical model and setup can predict the target or real response. According to AIAA (1998) the definition of the term "Validation" is:

"The process of determining the degree to which a model is an accurate representation of the real world from the perspective of the intended uses of the model." (AIAA, 1998)

3. Method

After a conversation with supervisor Tor Anders Nygaard this thesis was introduced. He is currently working at the wind department at IFE and had an interesting topic to offer. IFE needed a validation study on a current bridge project and this need were covered in this thesis. Before starting the simulations there were conducted a literature study to get a better view of previous work and gather information around this topic to get a better ground of comparison in the validation study.

The literature study was also used to gather academic knowledge around bridge girder construction and wind flow. After gathering enough knowledge and information the STAR CCM+ training started, to be able to do the simulations needed for the topic. A lot of time were used to gather information and knowledge, in addition to CAD-files and results for both bridge girders.

The next phase of the project was to conduct the needed simulations to see if the bridge girders from this thesis is compliable compared to similar bridge constructions, both theoretical and practical to see if the current bridge girder is valid.

3.1. Literature study

During the literature study different journals and theses on already developed and tested bridge constructions and bridge girders where studied. By studying older master theses about bridge constructions and bridge girders different focus and angles where shown and used in further work with this thesis. There are a lot of theses from different universities in Norway around this topic and most of them look at either Hardangerbrua or a planned bridge over Bjørnafjorden. Especially from the University in Stavanger there are many theses where Jasna Bogunovic Jakobsen is the supervisor which addresses bridge girder constructions and bridges at Bjørnafjorden and Hardangerfjorden the last 10 years.

Studies done in the earlier theses is studied and used as a guidance for work on this thesis. In addition is the references from earlier studies used as a base for better insight and knowledge at a basic level on this theme. After some research journals and theses from both Norway and the rest of the world where suggested as relevant studies for this thesis.

One of the most relevant thesis for this thesis was the doctorate thesis «Shaping effects on Aerodynamic of Long-Span Cable-Supported Bridge Deck by Unsteady RANS» (Haque, 2015) were studied. The doctorate thesis addresses a flow analysis on a bridge girder at different designs and how changes in the wind velocity and design affects how the wind flow behaves.

Where the pressure on the bridge girder is highest and how small design changes can make great impact on the results is also addressed. In this journal there were conducted a validation study of a bridge girder in comparison to a square and a rectangle. This results and reflection are also used as a basis in this thesis.

There were conducted searches in Google Scholar on "Tore Helgedagsrud", this search gave 16 results and all the results were relevant journals on bridge girders and flow in the same way as Haque's journal. The journal «Using ALE-VMS to compute aerodynamic derivatives of bridge section» (Helgedagsrud et al., 2018) in a good example on a journal by Tore Helgedagsrud that shows both design of a bridge girder and a flow analysis. Tore Helgedagsrud is a fellow at NTNU and has written many relevant analyses on bridge girder and his work is a good basis for the work on bridge girder in this thesis. Tore Helgedagsruds «Isogeometric Modeling and Experimental Investigation of Moving-Domain Bridge Aerodynamics» (Helgedagsrud et al., 2019) was also seen as a relevant paper. This paper is used for comparison in the analysis for different angles of attack.

A search on "Bridge Girders" in Science Direct and Web of Science gave few results, but those results gave a wider knowledge on what a bridge girder is and how it should be designed. One of the journals which was relevant in the search was «Investigation of flutter performance of a twin-box bridge girder at large angles of attack» (Tang et al., 2019). This journal addresses a double bridge-girder-bridge's aerodynamic behaviour from different wind angles of attack.

The literature study has led to a wider and deeper understanding of how bridge girders behave in relation to the bridge girders design and structure. The basis to conduct a validation study is better than before and the understanding and basis is better for the further work on this thesis. To form a better base for a validation study journals and theses on relevant bridges in Norway were studied and especially Hardangerbrua and the bridge over Lysefjorden are relevant. By conducting searches in «Google», «Science Direct», «Web of Science» and «Google Scholar» different journals that gave better understanding on how bridges are structured and which simulations that are most relevant for this thesis. It appears that there are some bridge building project going on in Norway today, and wind flow and bridge girder design is essential for all of them. Therefore, there are many possibilities for the conduction of the validation study.

To get the basic knowledge needed for this theses about bridge girders and aerodynamic forces the book «Theory of Bridge Aerodynamics» (Strømmen, 2010) was used as a reference. This book addresses the basic knowledge of the topic that this thesis is based on.

3.2.Result retrieval

Simulations will be conducted in this thesis, to get grounds for an analysis and discussion. The simulations will be conducted in the computer aided program STAR CCM+, which will be further discussed in the next chapter. By conducting simulations on two bridge girders and compare the results achieved in the simulations to previous work on bridge girders, the ground for validation and comparison is given. There will be conducted simulations on pressure, velocity, lift and drag on the different models, this will be explained deeper in the next chapters. There will be no focus on modelling in this thesis and the simulations will be based on CAD-files received from the project group at the Hardangerbrua project.

4. Simulation

To demonstrate how the wind behaves in relation to a geometry's design simulations are carried out in the computer aided program STAR CCM+. In this chapter there will first be an introduction to STAR CCM+ and its functions, before the simulations will be carried out in 2D for two dimensions of the same bridge girders with different inlet velocities. The results include pressure distribution and the resulting lift and drag forces as a function of angle of attack.

The analysis of the simulations presented in this chapter will be further looked at in the next chapter, and then discussed in chapter 6.

4.1. STAR-CCM+

In the implementation of the CFD simulations in this thesis the Computer Aided program STAR CCM+ was used. STAR CCM+ is a CAE (Computational Aided Engineering) solution for solving multidisciplinary problems in both fluid and solid continuum mechanics, within a single integrated user interface (Siemens, 2018).
The STAR-CCM+ simulation environment offers all stages required for carrying out engineering analyses, including:

- Import and creation of geometries
- Mesh generation
- Solution of the governing equations
- Analysis of results
- Automation of the simulation workflows for design exploration studies
- Connection to other CAE software for co-simulation analysis

4.2. Implementation of simulations

The first step of the simulation process is to make a 2D model of the bridge girder in STAR CCM+, then this 2D model is extracted to a 3D model. Making the bridge girder model in STAR CCM+ makes it easy to make small changes to the model without complications and it is easy to see the changes in wind and design. The next step is to apply mesh to the model before applying wind forces and direction. After applying the mesh, the 3D model is converted to a 2D model before running the simulations. Now the flow analysis is conducted, this analysis

shows how the lift and drag behaved dependent on the angle of attack and where most pressure is applied to the model.

Mesh

Meshing in simulation is the process of applying a web of small pieces on the model to conduct more accurate simulations. Smaller mesh pieces mean more concrete and realistic simulations, but it also makes the simulations more time consuming. In the simulations there will be used different sized levels of quadratic mesh as presented in Figure 4.1. This type of mesh is used in all the simulations conducted with STAR CCM+.

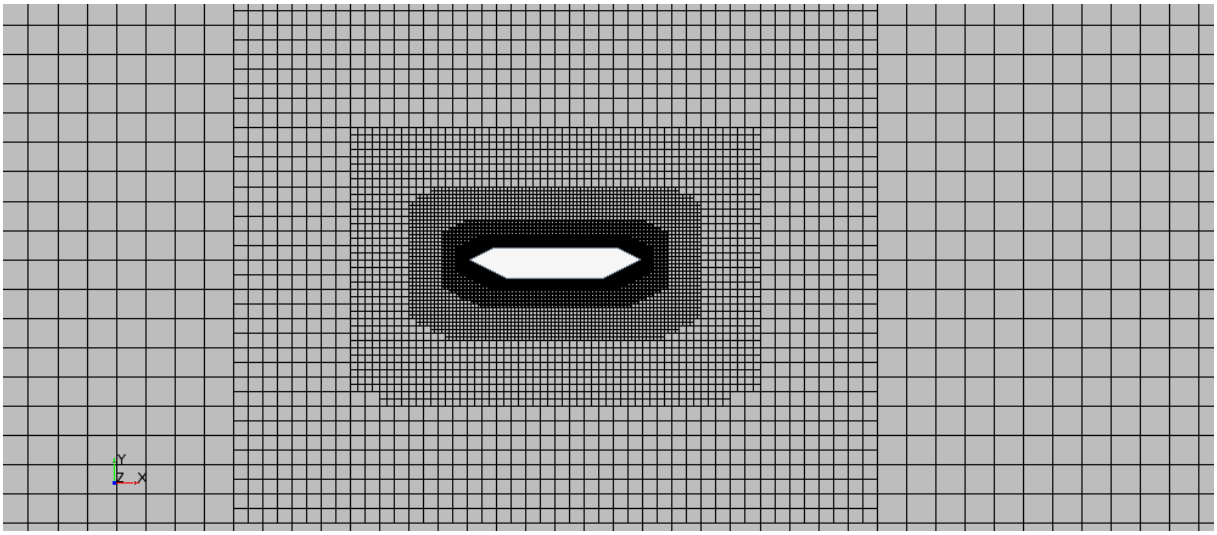

Figure 4.1: Meshed model with different layers of quadratic mesh from STAR CCM+

Computational Domain

When choosing the Computational Domain, the area where the calculations will be conducted, there are some factors to consider. From practical point of view, the domain should be as large as possible so that the boundary of the domain does not affect the response around the target object. According to Haque (2015) the size of the computational domain have been investigated to reduce uncertainty in the solution due to domain size.

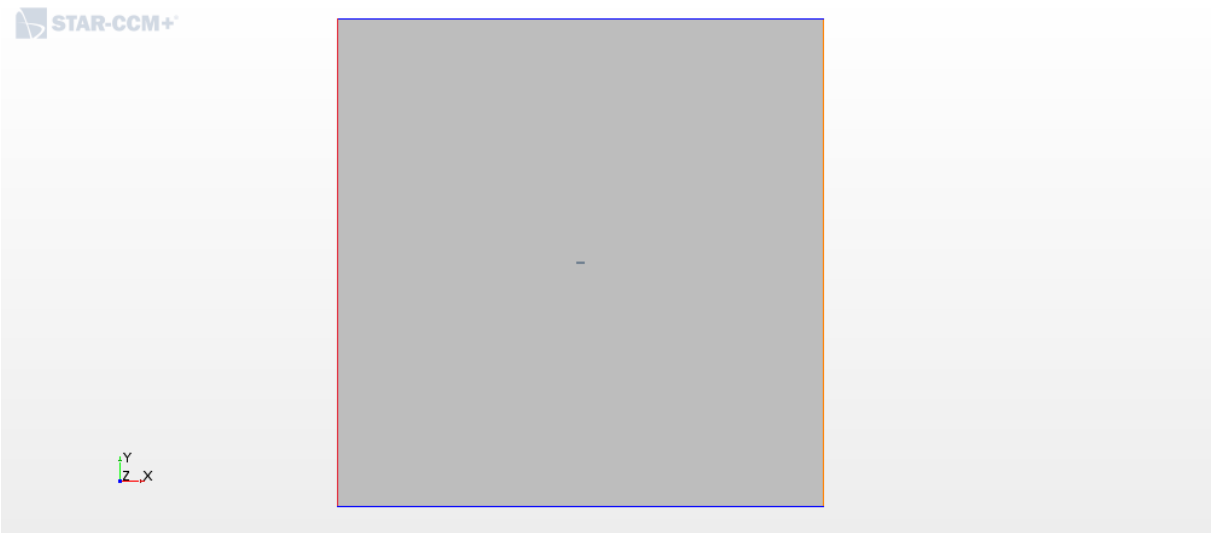

Figure 4.2: Computational domain for the bridge girder alternative 1 from STAR CCM+.

In Figure 4.2 the computational domain for the bridge girder alternative 1 is displayed. The pink area is the computational domain, and the white spot in the middle is the outline of the bridge girder. The figure shows the size of the computational domain in comparison with the bridge girder model. With a computational domain this big, the domain will most likely not have any negative impact on the bridge girder calculations.

2D and 3D modelling

The simulations were carried out on both two-dimensional (2D) and three-dimensional (3D) models. In a 2D-model only the x- and y- axis is taken into consideration, while in a 3D-model the z-axis is also considered. In this thesis there will only be conducted simulations on 2D models. The reason for this is that the simulations will be less time consuming, and the result from the 2D simulations are still valid and reliable for further analysis.

Pressure and velocity simulations

In the upcoming simulations the pressure and velocity will be analysed. The colour scale represents the size of the velocity and pressure. In the pressure simulation the reference pressure is 0 Pa, which means that the pressure illustrated as negative on the colour scale if the pressure lower than the reference pressure.

4.3.2D simulations

First there were conducted simulations in 2D of a square, rectangle and two different bridge girders. Then there were conducted simulations on six different angles of attack. The turbulence model used in all the simulations is the K-omega turbulence model from STAR CCM+. The Reynolds number for each simulation is calculated after the simulations. In all the wind flow simulations the wind is flowing from the left to the right.

4.3.1. 2D square and rectangle

Simulations on a square with sides 1m x 1m and a rectangle with sides 5m x 1m where conducted. Both geometries were modelled and then simulated in STAR CCM+.

Square

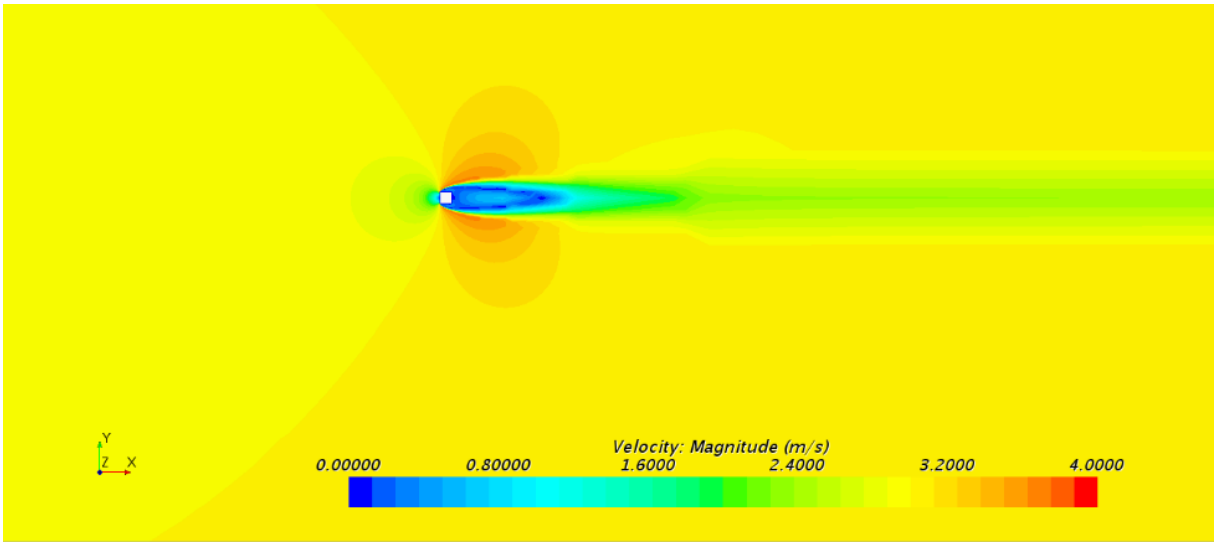

Figure 4.3: Square 2D velocity simulations from STAR CCM+.

Figure 4.3 displays a 2D model of a $1m^2$ square within the boundaries of the computational domain. From the flow patterns it is shown that the speed is lowest in the blue area right behind the square. The wind velocity was set to 3.0 m/s and the inlet flow is perpendicular to the square from the left. The yellow area represents a flow speed of 3.0 m/s and its seen be the red are that the flow is split, and the velocity increases around the square. The Reynolds number for the square is calculated to 200 000 using Eq 2-5.

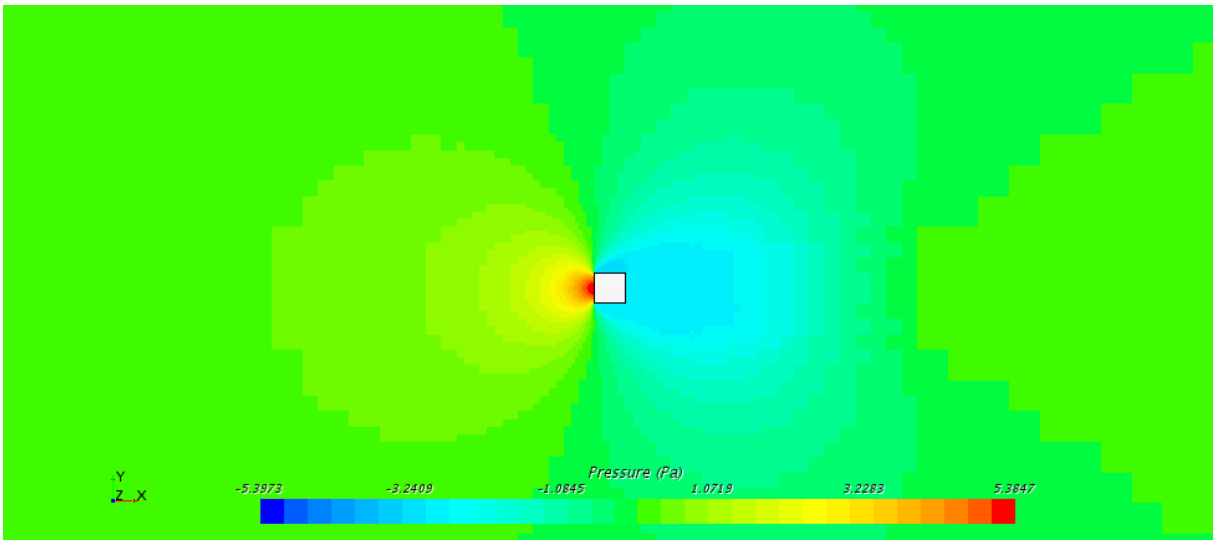

Figure 4.4: Square 2D pressure simulations from STAR CCM+.

Figure 4.4 presents the pressure simulation for the square. As shown from the red and yellow area the pressure is high on the inlet side of the square, on the outlet side of the square there is a lower pressure illustrated by the turquoise colour. The green area represents the reference pressure of 0 Pa. The pressure is high on the inlet side because the wind is coming in perpendicular to the square.

Rectangle

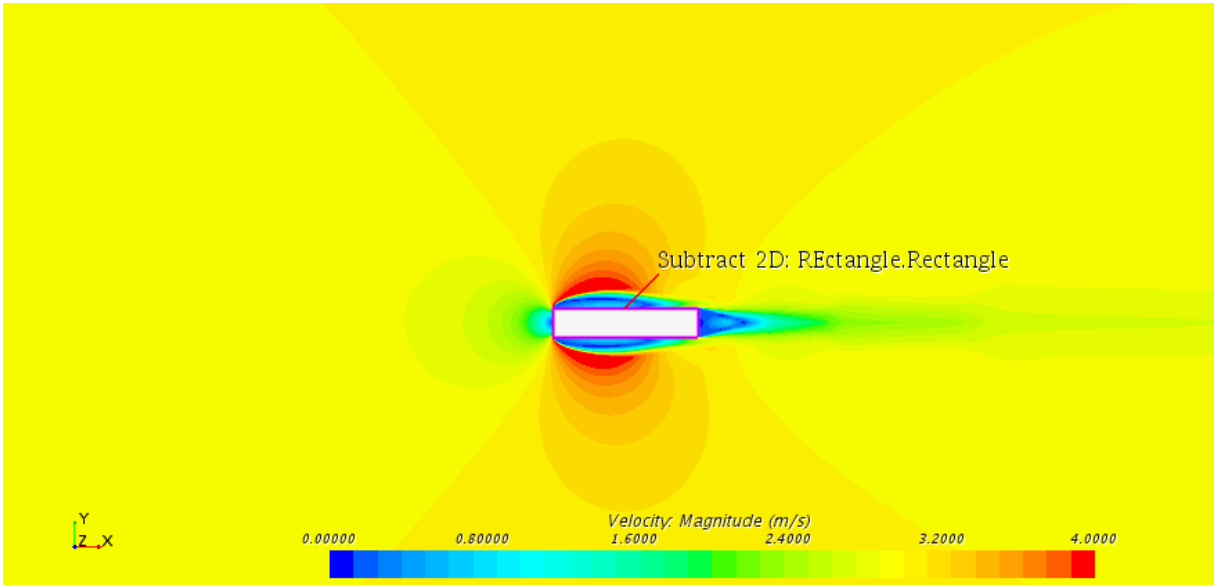

Figure 4.5: Rectangle 2D velocity simulations from STAR CCM+.

Figure 4.5 presents the simulations for the rectangle. As shown from this figure the wind velocity is highest around the inlet corners of the rectangle. The wind velocity was set to 3.0 m/s and the inlet flow is perpendicular to the rectangle. The Reynolds number for the rectangle is calculated to 340 000 using Eq 2-5.

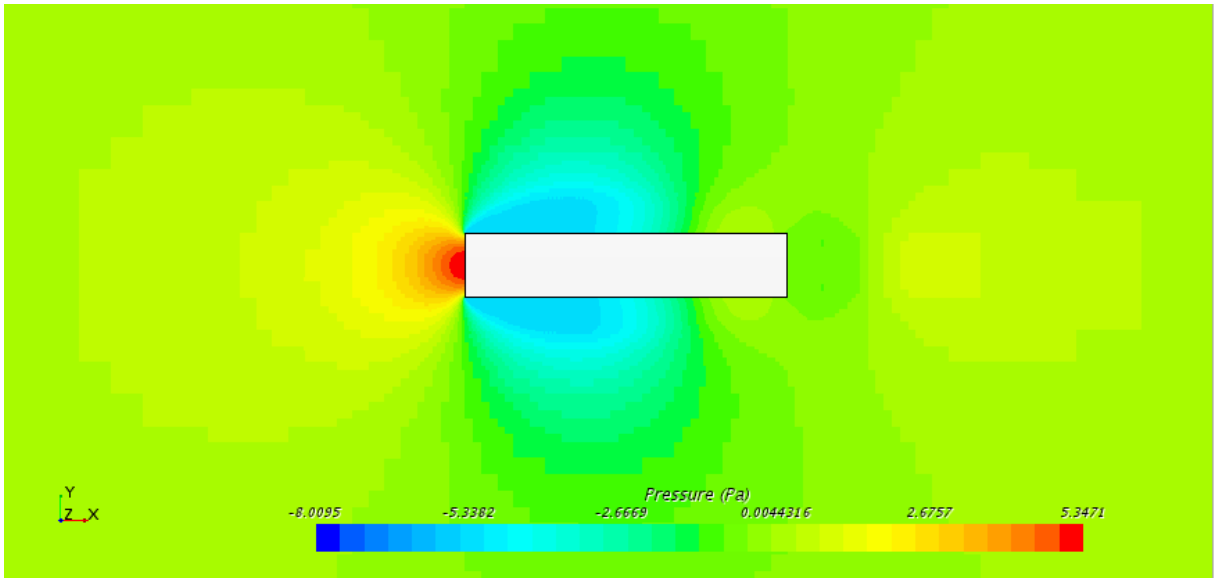

Figure 4.6: Pressure simulations of 2D rectangle from STAR CCM+.

Figure 4.6 presents the pressure simulation for the rectangle. The wind is coming in perpendicular on the rectangle and creates a high pressure on the inlet left side of the figure. This high pressure is illustrated by the red and yellow colour. When the wind flow reaches the rectangle, it is split into two flows and this creates a lower pressure around the bridge girder, illustrated by the turquoise field.

4.3.2. Bridge girder simulations with inlet velocity 3.0 m/s

The first alternative for the bridge girder is a simplified model of the bridge girder at Hardangerbrua. The dimensions for the bridge girder are given in Table 4.1 and the geometry is similar to the bridge girder in Figure 1.1. This bridge girder alternative 1 is analysed in relation to the bridge girder from (Haque, 2015) which is illustrated in Figure 5.5 and its dimensions are presented in Table 5.1. The bridge girder with 3.0 m/s inlet velocity will be called bridge girder alternative 1 after this.

Table 4.1: Bridge girder alternative 1 with 3.0 m/s inlet velocity's dimensions.

B	0.26 m
b	0.21 m
H	0.05 m
W	$\frac{b}{B} = \frac{0.21}{0.26} = 0.81$

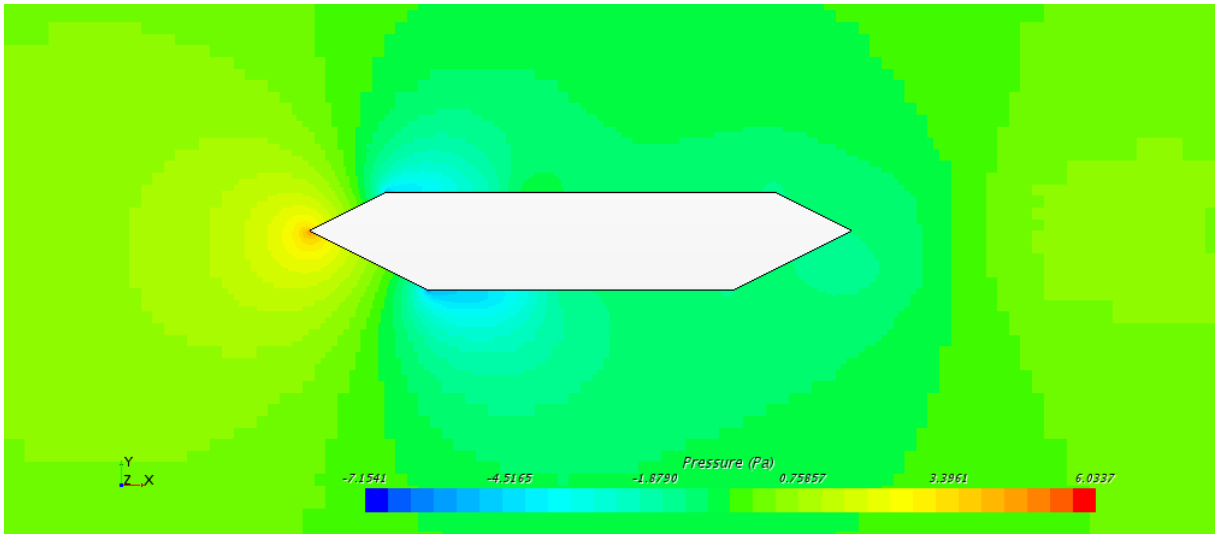

Figure 4.7: Pressure simulations for 2D bridge girder with inlet wind velocity 3.0 m/s from STAR CCM+.

Figure 4.7 presents the pressure simulations conducted on the 2D model of bridge girder alternative 1. The pressure is highest at the inlet of the bridge girder (at the left side). The high pressure is displayed with the red colour. Low pressure around the left upper and lower corner is created because of the inlet wind flow that is split when hitting the bridge girder and creating the lower pressure.

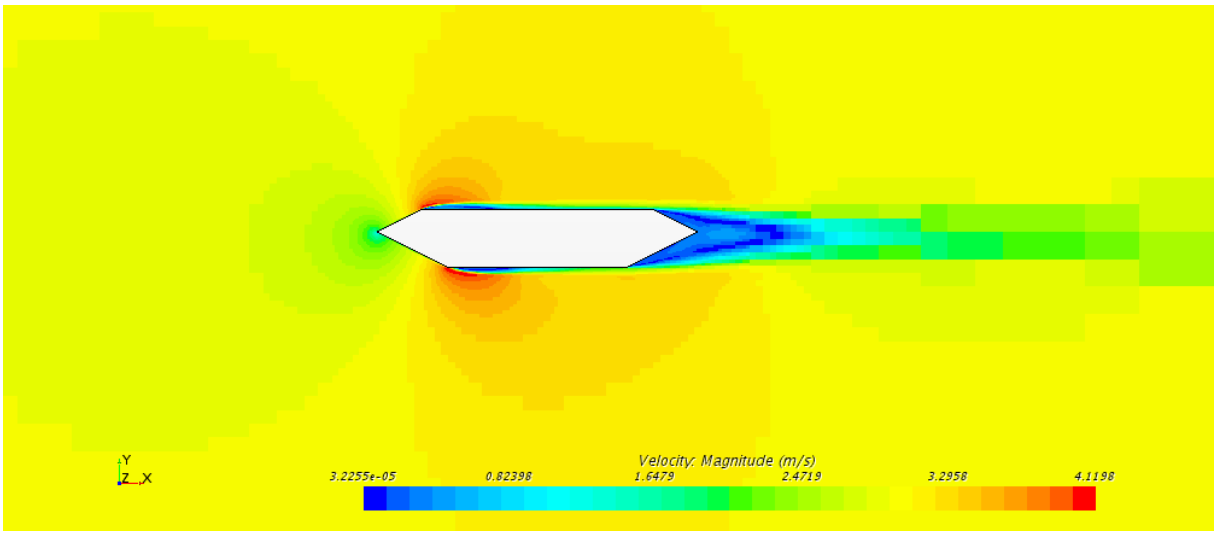

Figure 4.8: Velocity simulations of 2D bridge girder with inlet wind velocity 3.0 m/s from STAR CCM+.

Figure 4.8 presents the air velocity simulations of the bridge girder alternative 1. The inlet air velocity was set to 3.0 m/s. The highest velocity is on the upper and lower left side corner, this is shown by the red color. The blue area on the back of the bridge girder demonstrates the low speed that accurs right after the wind has passed the girder because the wind is coming in perpindicular and the bridge girder is slowing the wind down. Using the formula for Reynold number (Eq 2-5) a Reynolds number of 17 000 is calculated for this bridge girder. The high Reynolds number means that the wind flow is turbulent.

4.3.3. Bridge girder with inlet velocity 8.0 m/s

For the upcoming simulations the velocity is set to 8.0 m/s. This is because the comparative data is analysed with an inlet velocity of 8.0 m/s. The bridge girder with 8.0 m/s inlet velocity will be called bridge girder alternative 2 after this.

The bridge girder used in the last chapter had a small geometry and for the simulations in this chapter the model is scaled 50:1. This gives the dimensions shown in Table 4.2. The scaling was done so the dimensions would be comparable to the bridge girder in (Helgedagsrud et al., 2019).

Table 4.2: Bridge girder alternative 2 with 8.0 m/s inlet velocity's dimensions.

B	13 m
b	10.5 m
H	4.25 m
W	$\frac{b}{B} = \frac{10.5}{13} = 0.81$

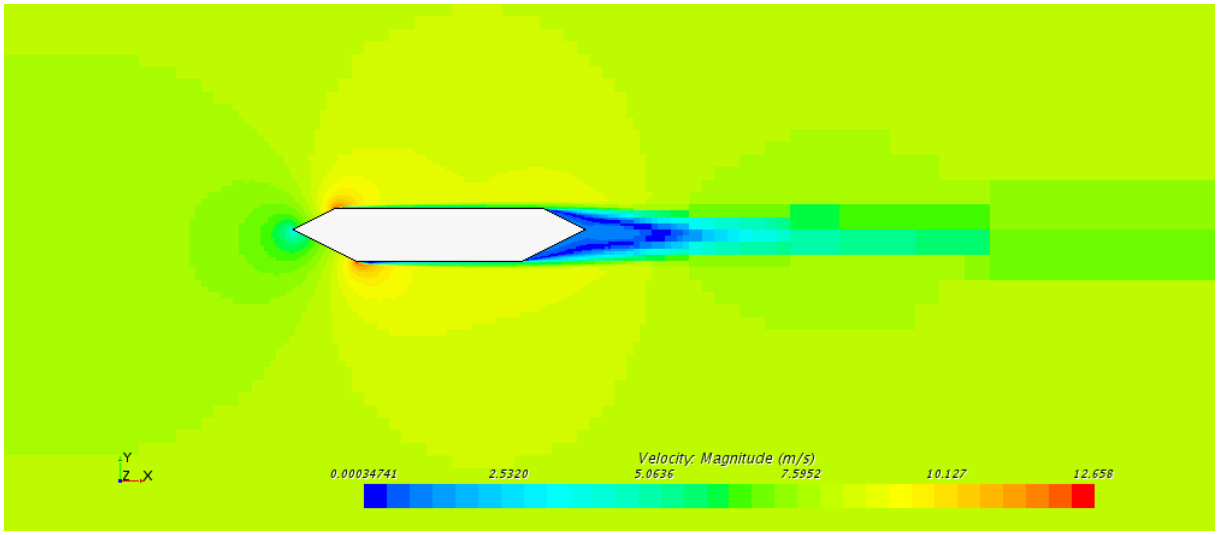

Figure 4.9: Velocity simulations of 2D bridge girder with inlet wind velocity 8.0 m/s from STAR CCM+

Figure 4.9 presents the air velocity simualtions for the bridge girder alternative 2. The air inlet velocity was set to 8.0 m/s. The wind is flowing in perpendicular to the bidge girder and this is shown by the tuquoise colour on the left tip of the bridge girder. The upper and lower left corner makes a split in the wind flow an the velocity increases shown by the red colouring. The Reynolds number for this bridge girder is 2 223 676, calculated with Eq 2-5.

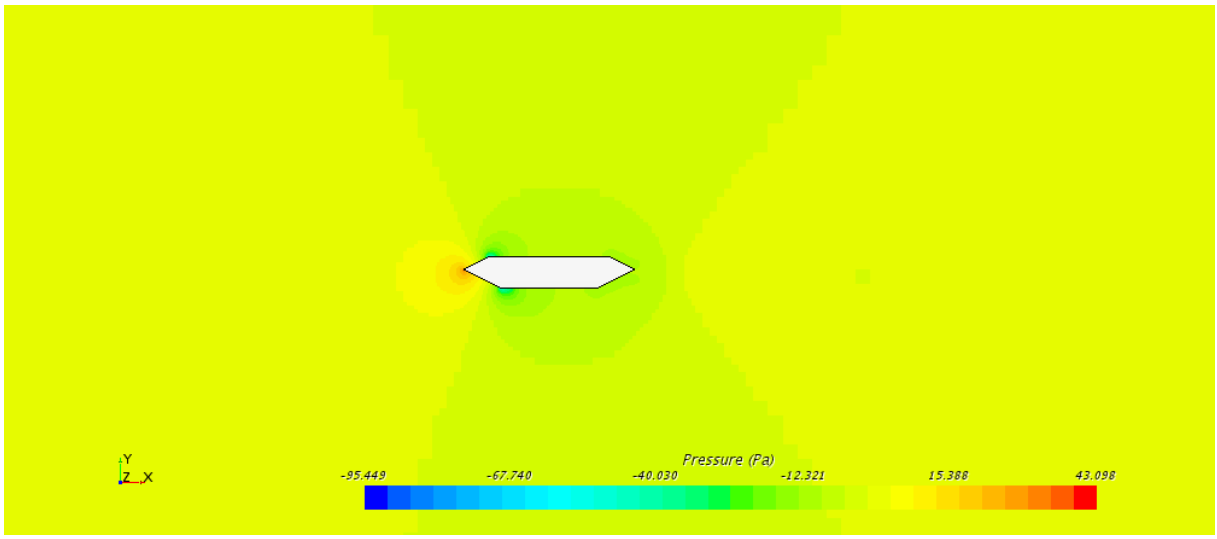

Figure 4.10: Pressure simulations of 2D bridge girder with inlet wind velocity 8.0 m/s from STAR CCM+

Figure 4.10 presents the pressure plot for the bridge girder with inlet velocity 8.0 m/s. The angle of attack in this case is 0 degrees and the pressure is even over and under the bridge girder shown by the green area around the bridge girder. The pressure on the left tip is higher because this is where the inlet air flow hits the bridge girder. Low pressure around the left upper and lower corner is created because of the inlet wind flow that is split when hitting the bridge girder and creating the lower pressure.

4.4.Lift and drag vs. angle of attack

To see how the bridge behaves in different wind angles there are conducted lift and drag force simulations. So far in the simulations an angle of attack of 0 degrees is analysed. Now there will be conducted simulations in STAR CCM+ for 3 degrees, -3 degrees, -5 degrees, -7 degrees and -10 degrees for the angle of attack. The simulations with different angles of attack are only conducted on the second alternative for the bridge girder. Alternative 2 has the most comparable data, and on this bridge girder small angles of attack will have impact on the results worth analysing. All the angles have a positive x-velocity of 8.0 m/s. the different inlet angles of attack is created by changing the y-direction inlet velocity.

3 degrees

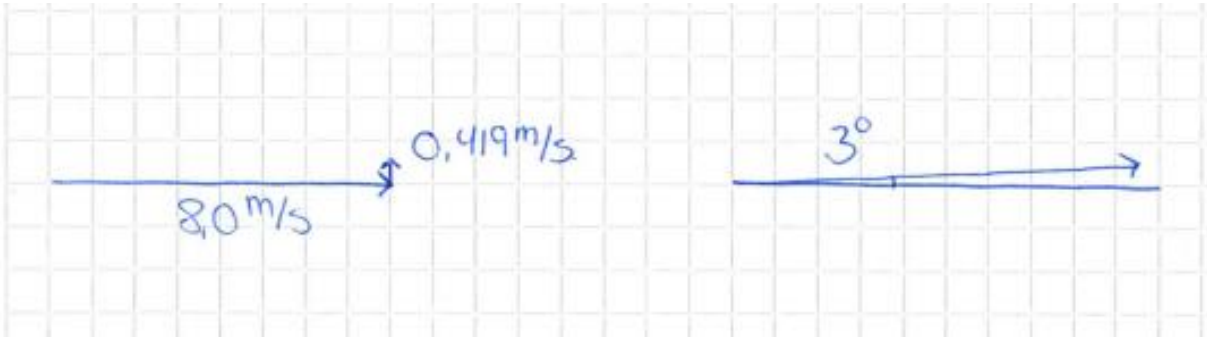

Figure 4.11: x- and y- velocity and direction for the 3 degrees angle of attack.

For the angle of 3 degrees it is applied a positive y-velocity of 0.419 m/s as shown in Figure 4.11. In this case the inlet speed is 8.011 m/s

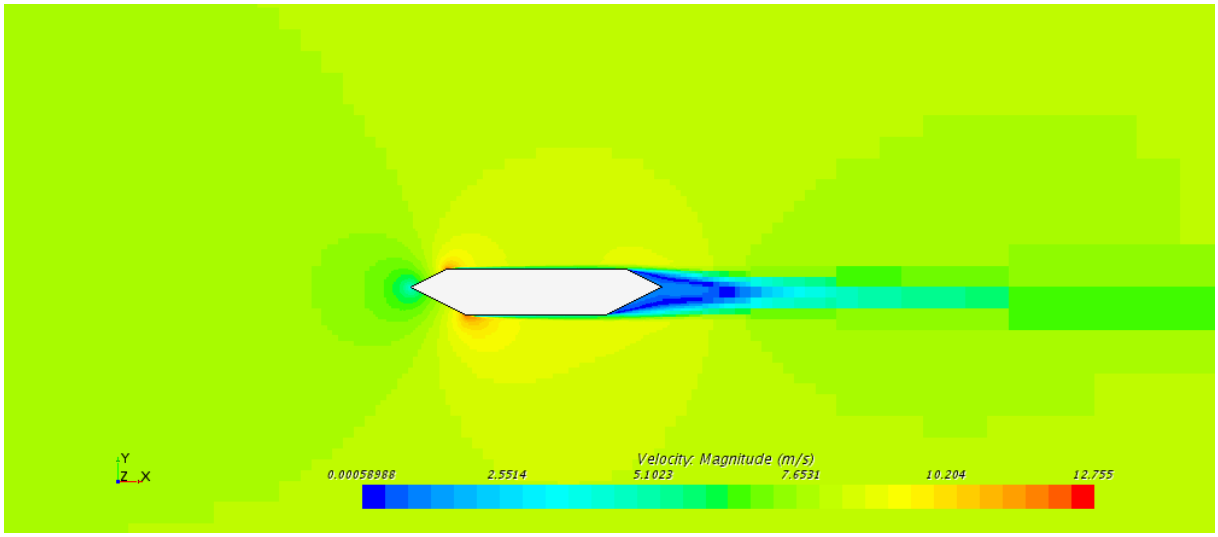

Figure 4.12: Velocity simulations of 2D bridge girder alternative 2 with a 3 degrees wind angle of attack from STAR CCM+.

Figure 4.12 presents the velocity simulations for the bridge girder with 3 degrees angle of attack. As demonstrated in Figure 4.11 the inlet velocity is flowing slightly upwards and this creates higher velocity around the left upper and lower corners. The velocity on the right side has a low velocity and this is illustrated by the blue area. The Reynolds number for this velocity is 2 226 733 calculated with Eq 2-5.

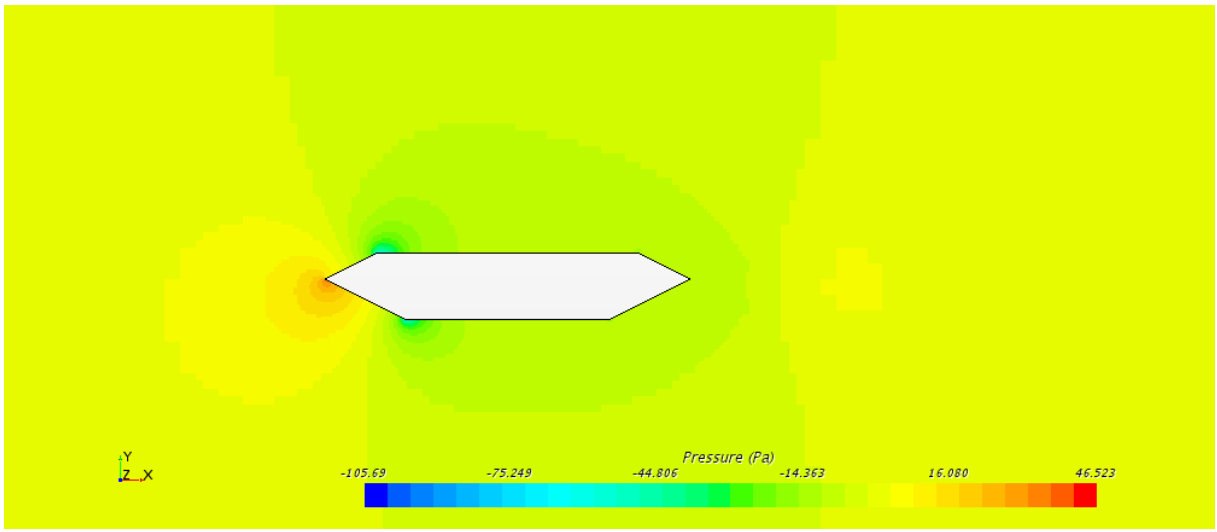

Figure 4.13: Pressure simulations of 2D bridge girder alternative 2 with a 3 degrees wind angle of attack from STAR CCM+.

Figure 4.13 presents the pressure simulations for the bridge girder with 3 degrees angle of attack. The wind flow is coming in on the left tip and creates the pressure shown by the orange/red colouring. When the wind is coming in from 3 degrees it is split and creates the low pressure on the upper and lower corners on the bridge girder.

-3 degrees

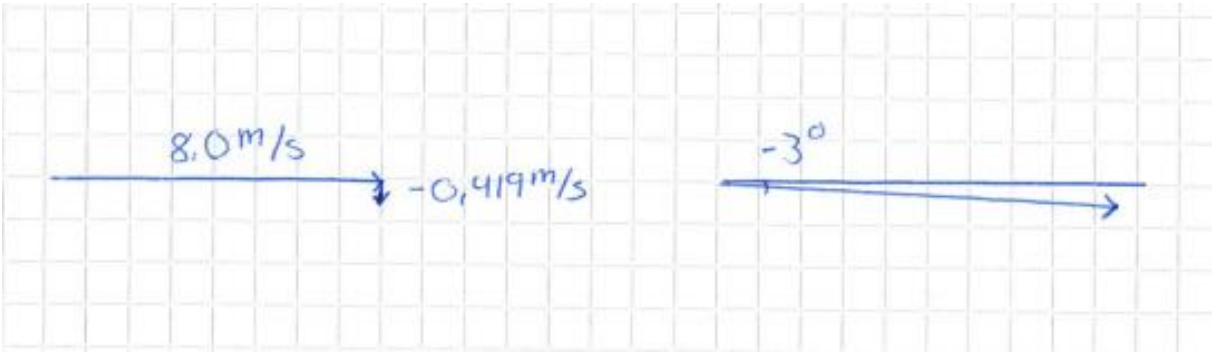

Figure 4.14: x- and y- velocity and direction for the -3 degrees angle of attack.

For the angle of -3 degrees it is applied a negative y-velocity of 0.419 m/s as shown in Figure 4.14. In this case the inlet speed is 8.01 m/s

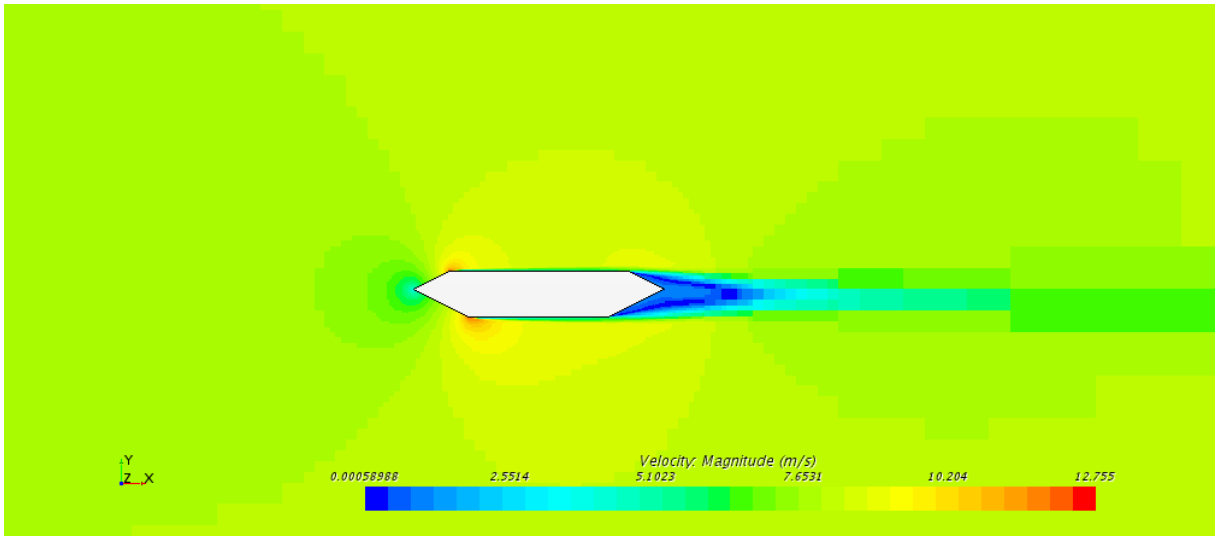

Figure 4.15: Velocity simulations of 2D bridge girder alternative 2 with a -3 degrees wind angle of attack from STAR CCM+.

Figure 4.15 presents the velocity simulations for the bridge girder with angle of attack -3 degrees. Figure 4.14 illustrates the inlet angle of attack and the blue area on the right side of the bridge girder is moving slightly downward. On the upper and lower left corners there are an increase in velocity shown by the red colour, while on the left tip there are a velocity decrease caused when the air hits the bridge girder. The Reynolds number for this velocity is 2 226 733 calculated with Eq 2-5.

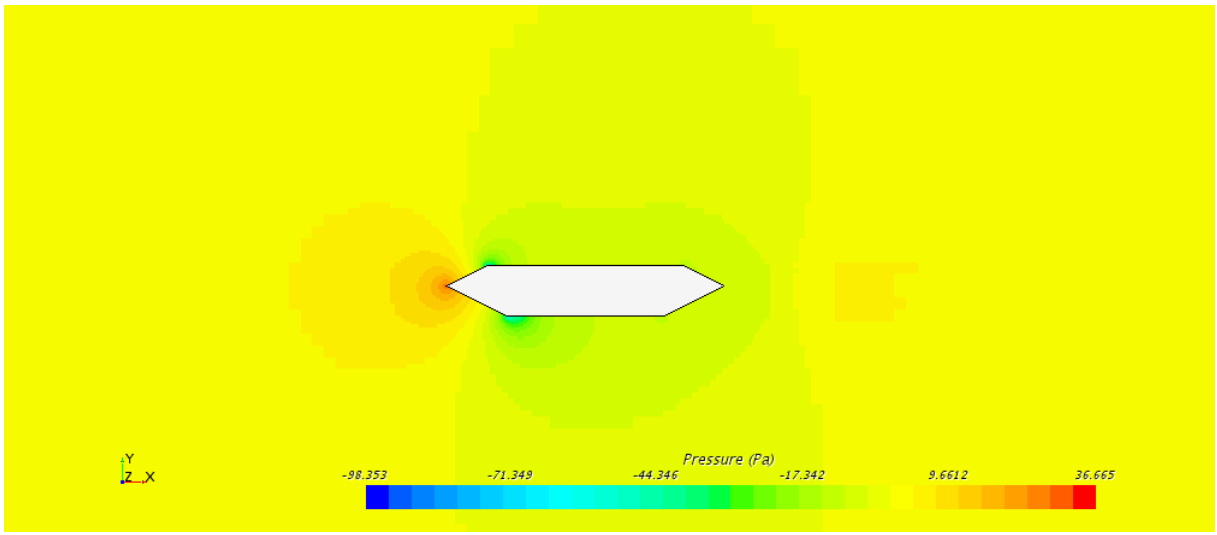

Figure 4.16: Pressure simulations of 2D bridge girder alternative 2 with a -3 degrees wind angle of attack from STAR CCM+.

Figure 4.16 presents the pressure simulations for the bridge girder with angle of attack -3 degrees. The pressure in this case is similar to the one for 3 degrees angle of attack, but on the left side tip the pressure is different. Since the wind is coming in slightly downwards in this case, as shown in Figure 4.14, the pressure is highest at the top of the inlet tip, while the pressure around the bridge girder is equally divided, illustrated by the green colouring. There is created a lower pressure around the upper and lower corner because of the flow free space created behind the corners.

-5 degrees

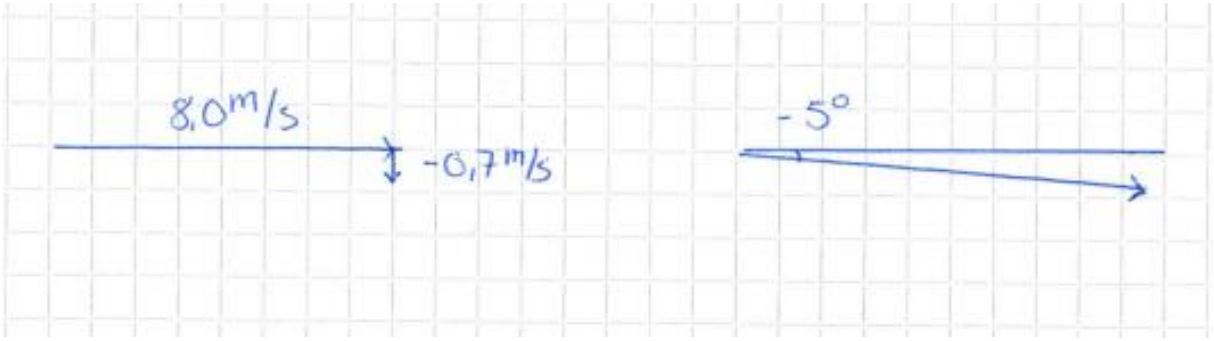

Figure 4.17: x- and y- velocity and direction for the -5 degrees angle of attack.

For the angle of -5 degrees it is applied a negative y-velocity of 0.7 m/s as shown in Figure 4.17. In this case the inlet speed is 8.03 m/s

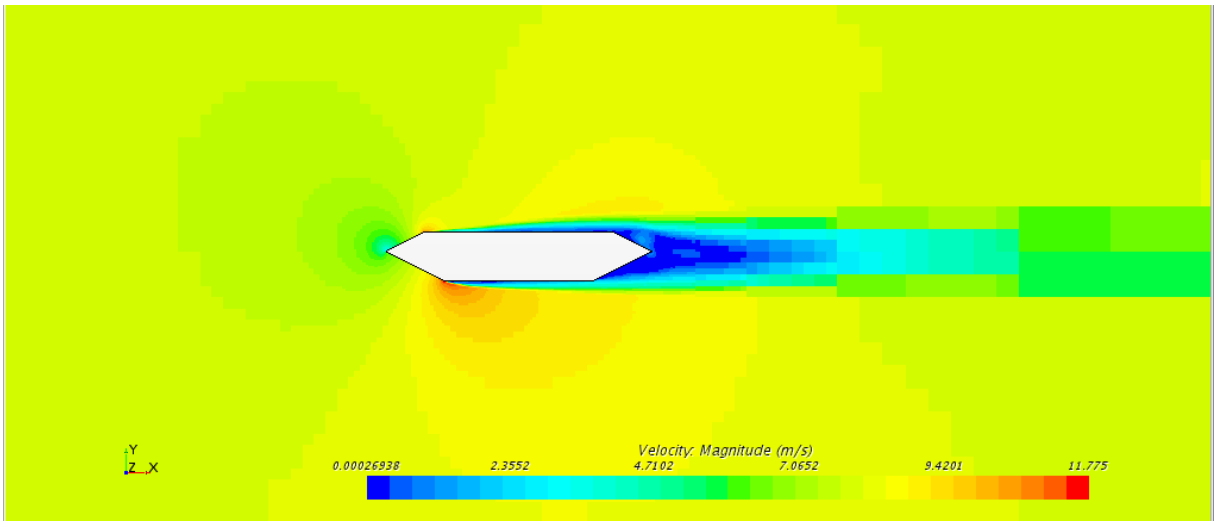

Figure 4.18: Velocity simulations of 2D bridge girder alternative 2 with a -5 degrees wind angle of attack from STAR CCM+.

Figure 4.18 presents the velocity simulations for the bridge girder with angle of attack -5 degrees. For -5 degrees angle of attack the wind is coming in slightly downwards, as shown in Figure 4.17, and this can be seen by the blue area on the right side of the bridge girder where the blue field is slightly pointing downwards. On the left corner underneath the bridge girder the wind flow is slit and the velocity increases, shown by the red colouring, and the same thing happens on the upper left corner. The Reynolds number for this velocity is 2 232 014 calculated with Eq 2-5.

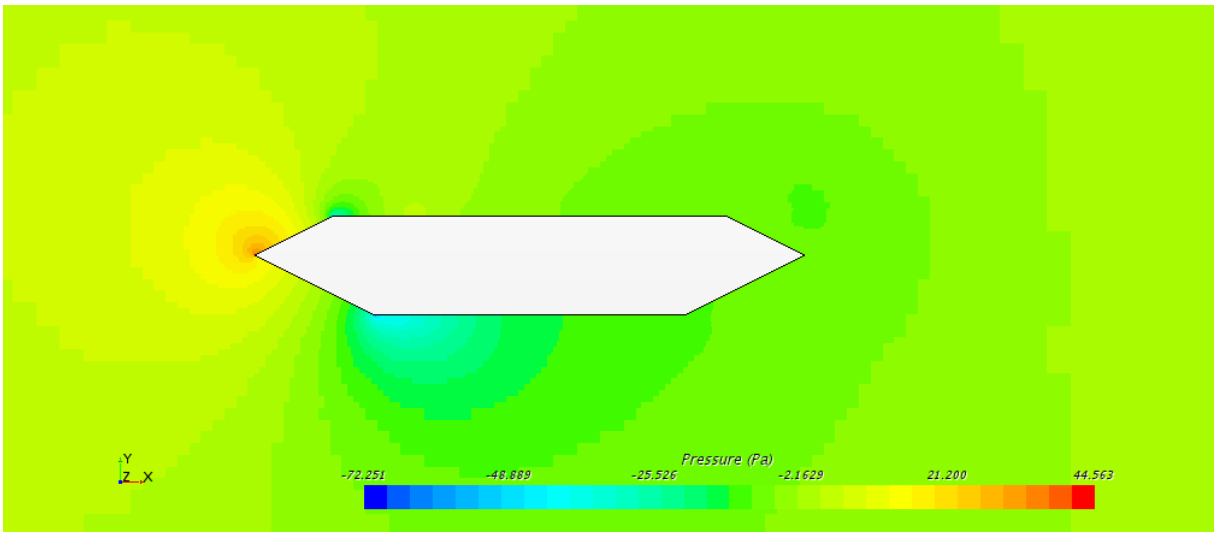

Figure 4.19: Pressure simulations of 2D bridge girder alternative 2 with a -5 degrees wind angle of attack from STAR CCM+.

Figure 4.19 presents the pressure simulations for the bridge girder with -5 degrees angle of attack. The pressure is highest on the left tip of the bridge girder. This is where the inlet air flow hits the bridge girder, and creates the high pressure, underneath the bridge girder the pressure is lower, due to the lack of wind flow on the turquoise area.

-7 degrees

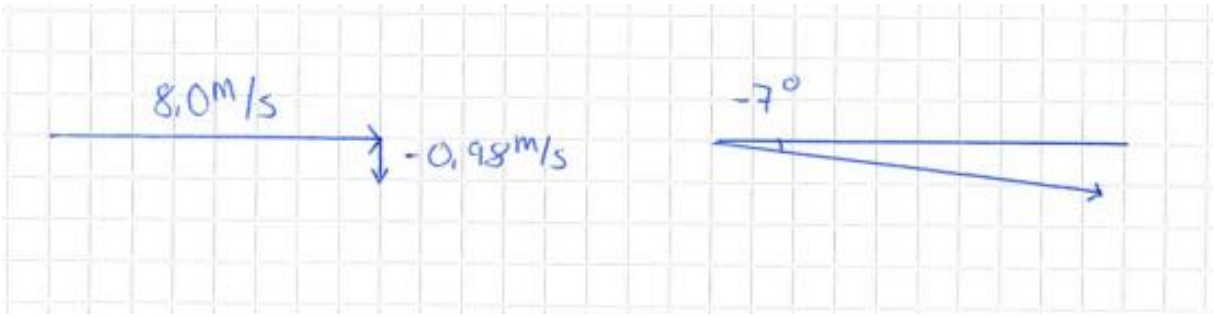

Figure 4.20: x- and y- velocity and direction for the -7 degrees angle of attack.

For the angle of -7 degrees it is applied a negative y-velocity of 0.98 m/s as shown in Figure 4.20. In this case the inlet speed is 8.06 m/s

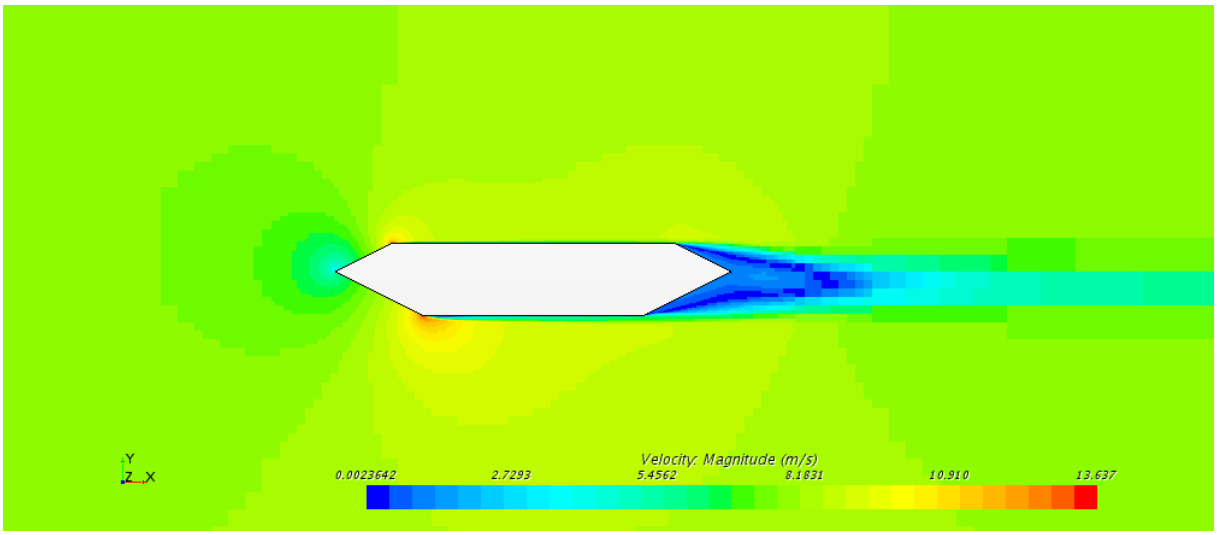

Figure 4.21: Velocity simulations of 2D bridge girder alternative 2 with a -7 degrees wind angle of attack from STAR CCM+.

Figure 4.21 presents the velocity simulations for the bridge girder with -7 degrees angle of attack. For this angle of attack the wind is coming in slightly more downwards, as illustrated in Figure 4.20, and this can be seen by the blue colour on the right side of the bridge girder. Around the left corners there are created an increased velocity because of the split in the inlet flow. The Reynolds number for this velocity is 2 240 353 calculated with Eq 2-5.

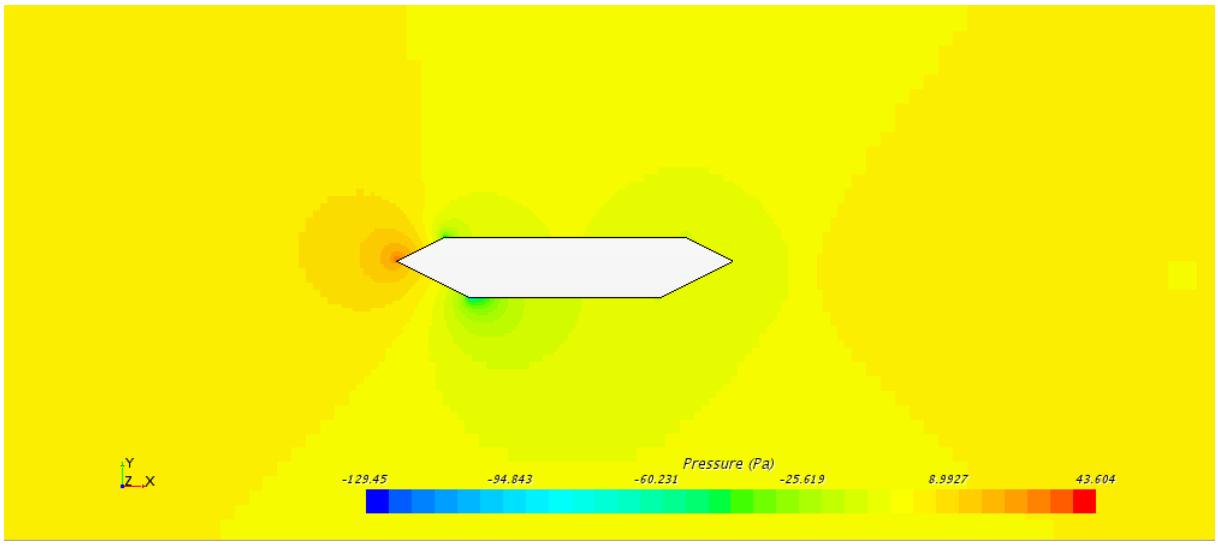

Figure 4.22: Pressure simulations of 2D bridge girder alternative 2 with a -7 degrees wind angle of attack from STAR CCM+.

Figure 4.22 presents the pressure simulations for the bridge girder with -7 degrees angle of attack. For this bridge girder the inlet pressure on the left tip is the highest. There are created a lower pressure around the left corners because of the wind flow flowing around the bridge girder.

-10 degrees

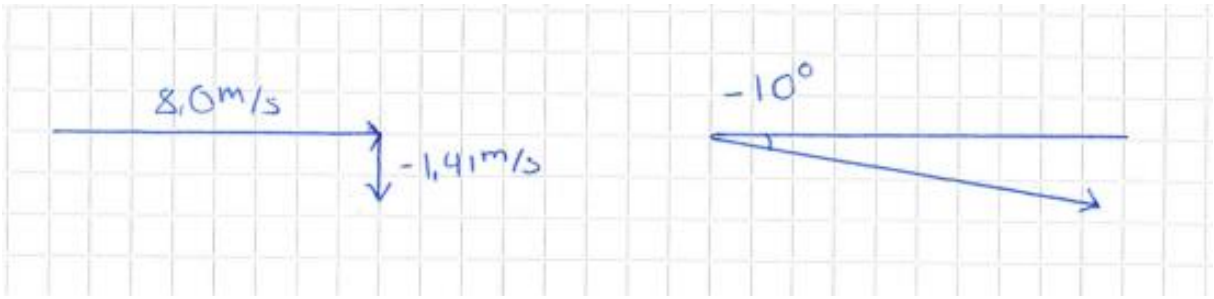

Figure 4.23: x- and y- velocity and direction for the -10 degrees angle of attack.

For the angle of -10 degrees it is applied a negative y-velocity of 1.41 m/s as shown in Figure 4.23. In this case the inlet speed is 8.12 m/s

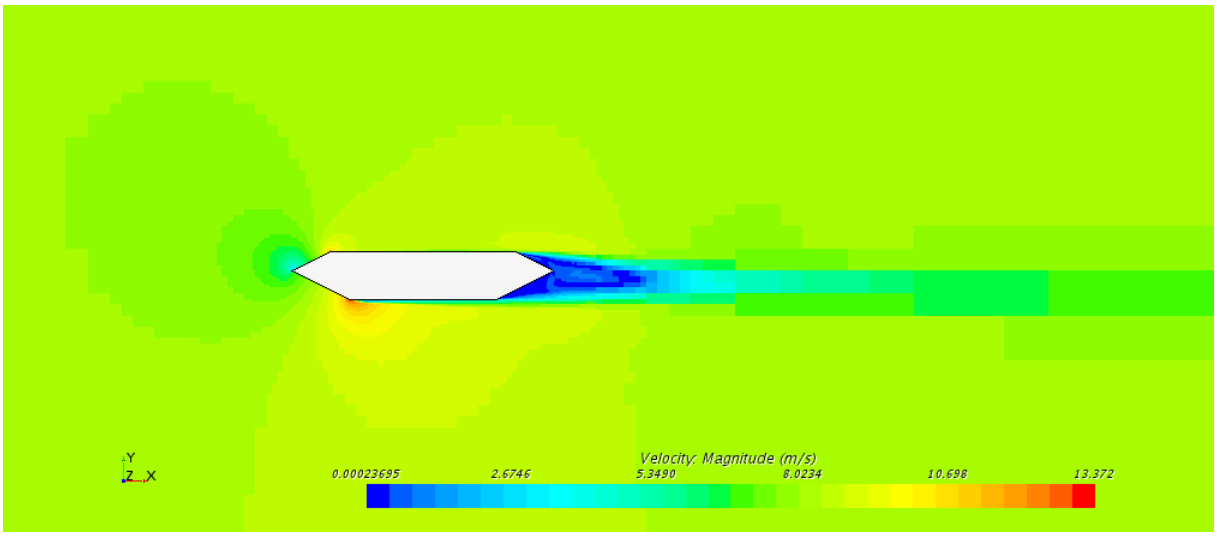

Figure 4.24: Velocity simulations of 2D bridge girder alternative 2 with a -10 degrees wind angle of attack from STAR CCM+.

Figure 4.24 presents the velocity simulations for the bridge girder with -10 degrees angle of attack. For this angle of attack the wind is coming in slightly more downwards, as illustrated in Figure 4.23, and this can be seen by the blue colour on the right side of the bridge girder where the field is pushed slightly downwards. Around the left corners there are created an increased velocity because of the split in the inlet flow. The Reynolds number for this velocity is 2 257 031 calculated with Eq 2-5.

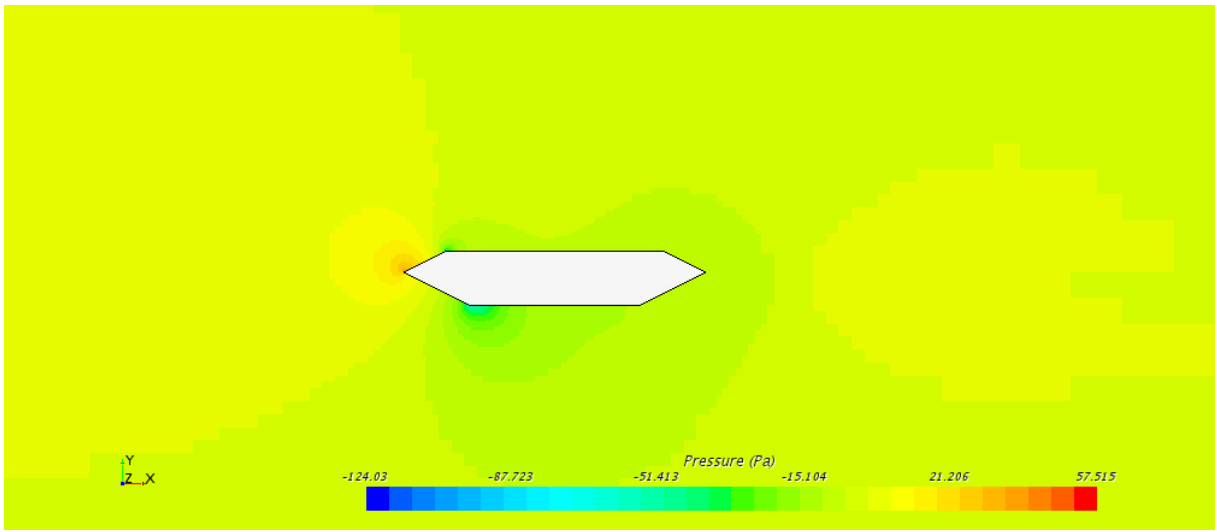

Figure 4.25: Pressure simulations of 2D bridge girder alternative 2 with a -10 degrees wind angle of attack from STAR CCM+.

Figure 4.25 presents the pressure simulations for the bridge girder with -10 degrees angle of attack. The pressure is highest around the left tip where the inlet flow hits the bridge girder and when the wind flow hits the upper and lower corners a lower pressure is created right after the wind has passed the corners. This low pressure is illustrated by the turquoise colour.

..

5. Results

In this chapter the simulations from chapter 4 will be analysed and seen in relation to earlier analyses and simulations. There will be conducted pressure analysis for the square, rectangle and the bridge girder alternative 1 and lift and drag analyses for the bridge girder alternative 2. The bridge girder alternative 1 and 2 models take basis in the same model, but in the second alternative the model is scaled 50:1 in relation to alternative 1.

The pressure analyses are compared to the simulations from (Haque, 2015), and this data is called “Experimental data” in the analyses.
Figure 5.1 and Figure 5.3 shows the measures used to conduct the simulations in (Haque, 2015) and how the sides are numbered in the analysis. The data from this thesis is normalized so the comparison is based on similar grounds.

The bridge girder alternative 2 is compared to (Helgedagsrud et al., 2019). Here the different angles of attack are analysed, and the lift and drag behaviour is presented in this chapter. The results for this comparison are prepared in Excel and the drag and lift coefficient is displayed later in this chapter.

The results presented in this chapter will be discussed in the next chapter.

5.1.2D square

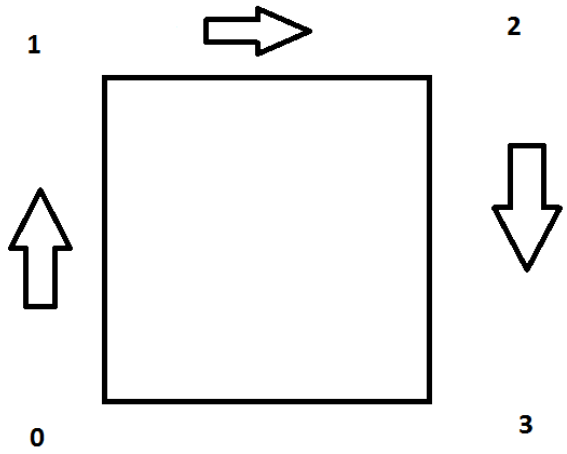

Figure 5.1: Sketch of square, with the total length for the simulations displayed.

In the 2D square simulations the data from (Haque, 2015) and the length values from the STAR CCM+ simulations had to be normalized to get Cp on the y-axis instead of pressure. This was done using this formula:

$$Cp = \frac{p}{0.5 * \rho * v^2} \qquad \textit{Eq 5-1}$$

Cp is calculated using Eq 5-1 and is the mean surface pressure coefficient and p is the pressure. The boundary conditions used in the simulations for velocity, v, is 3.0 m/s and the inlet air density, ρ, are 1.15 kg/m^3. As can be seen in Figure 5.1 the analysis is only valid for the inlet (0-1), top (1-2) and outlet (2-3) sides of the square. And the calculations to normalize the results is made for each part.

In Figure 5.2 the simulations conducted in this thesis is square_x and square_y. It is the same simulations, but the results are extracted for the y and x sides of the square. Here square_y are the inlet and outlet sides (0-1 and 2-3), while square_x is the top side of the square (1-2).

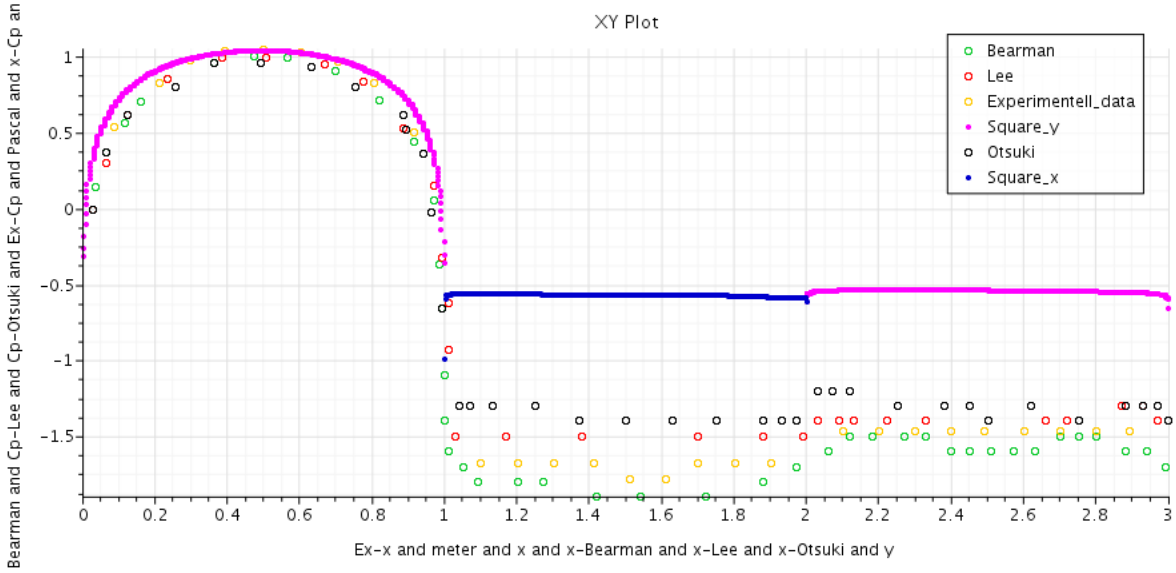

Figure 5.2: 2D model of square in comparison to the square from (Haque, 2015). The graphics is plotted in STAR CCM+.

Figure 5.2 shows that there is good compliance between the simulations and the experimental data in the points 0 to 1 in x-direction, but between 1 and 3 the compliance is not so good. The experimental data are shown by the yellow dots, and the Bearman (Bearman & Obasaju, 1982), Lee (Lee, 1975) and Otsuki (Ohtsuki, 1978) data represents initial data used in Haque (2015).

5.2.2D rectangle

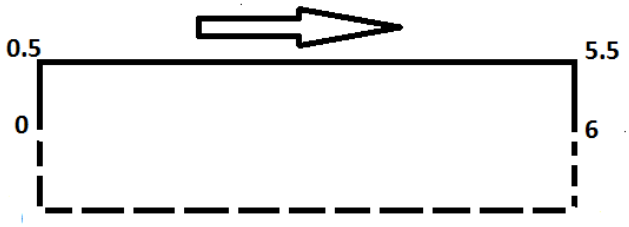

Figure 5.3: Sketch of rectangle, with the total length for the simulations displayed.

When normalizing the data for the rectangle, Eq 5-1 is used. Figure 5.3 shows that the rectangle in (Haque, 2015) was split into three lengths and only half of the rectangle were analysed. So, in the analysis for this thesis the same splitting was done, so the results could be compared. As for the square, the Cp is calculated using Eq 5-1.

Cp is the mean surface pressure coefficient and p is the pressure. The boundary conditions used in the simulations for velocity, v, is 3.0 m/s and the inlet air density, ρ, are 1.15 kg/m^3. As can be seen in Figure 5.3 the analysis is only valid for the inlet (0-0.5), top (0.5-5.5) and outlet (5.5-6) sides of the rectangle. And the calculations to normalize the results is made for each part.

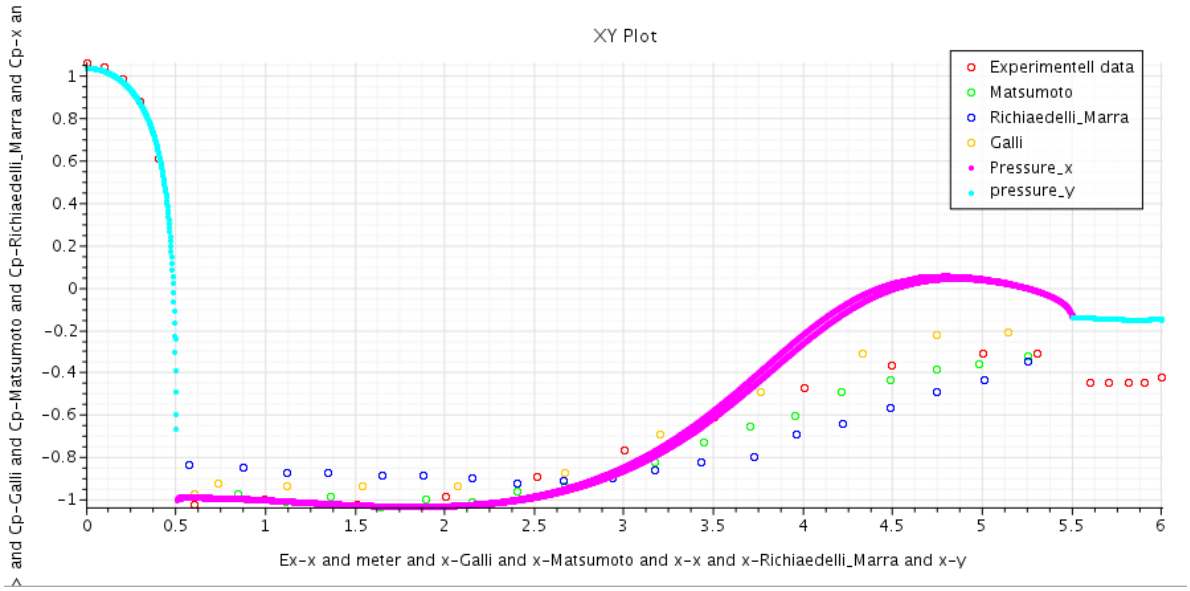

Figure 5.4: 2D model of rectangle in comparison to the rectangle from (Haque, 2015). The graphics is plotted in STAR CCM+.

Figure 5.4 shows that there is good compliance between the pressure in the experimental data and in the simulations conducted in this thesis from 0 to 3, between 3 and 6 the compliance between the simulations and the experimental data are not that good. The experimental data are shown by the red dots, and the Matsumoto ((Mannini et al., 2010) and (Matsumoto et al., 2003)), Galli (Galli, 2005) and Richiaedelli and Marra (Ricciardelli & Marra, 2008) represents initial data used in (Haque, 2015).

5.3.Bridge girder 2D

The two bridge girders that are analysed are both initially the same bridge girder, but with different dimensions. The bridge girder is a model for Hardangerbrua.

Bridge girder alternative 1

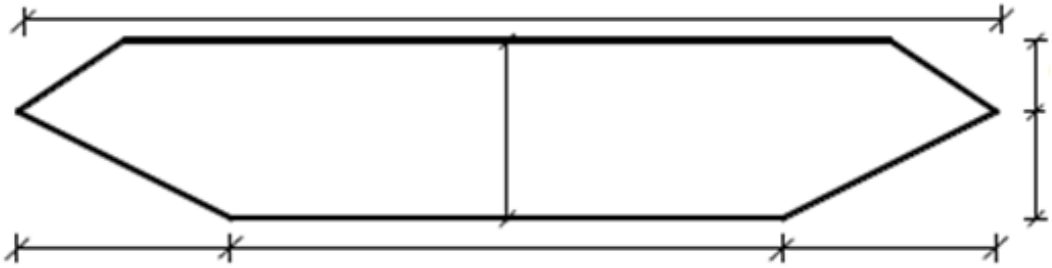

Figure 5.5: Bridge girder design for the girder from the PhD thesis (Haque, 2015).

Figure 5.5 illustrates the bride girder from (Haque, 2015) that are used as a comparison for the simulations on bridge girder alternative 1 in this thesis. The dimensions for Figure 5.5 are presented in Table 5.1.

Table 5.1: Dimensions for (Haque, 2015) bridge girder

B	5.5 m
b	3.5 m
H	1 m
W	$\frac{b}{B} = \frac{3.5}{5.5} = 0.64$

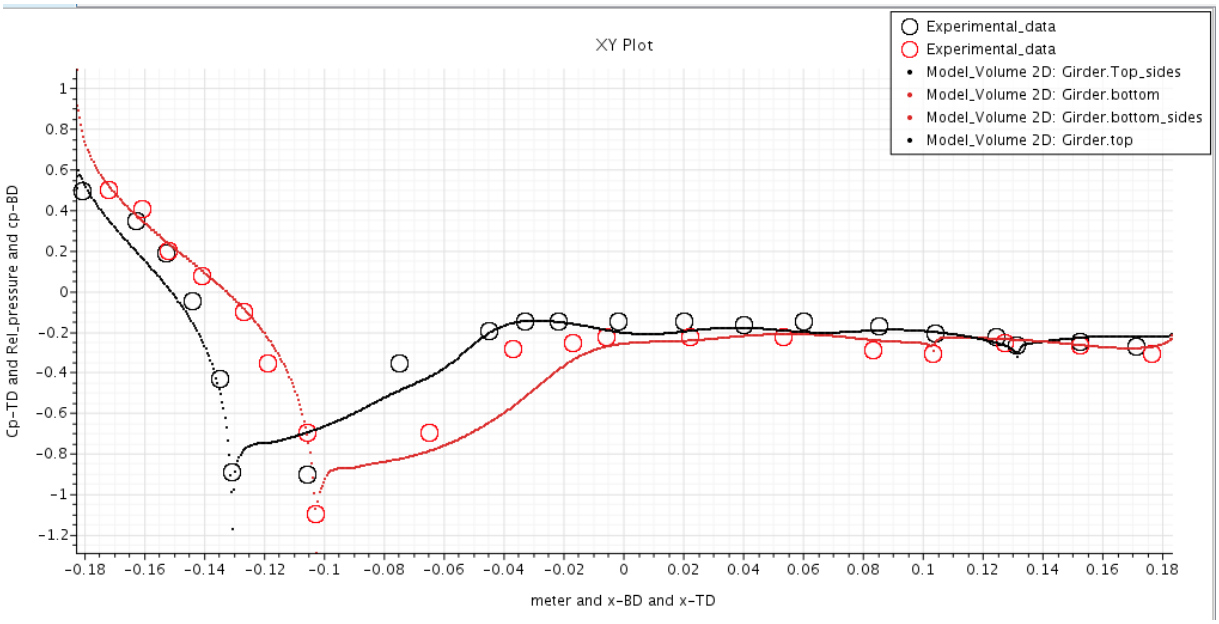

Figure 5.6: 2D model of bridge girder alternative 1 in comparison to the bridge girder from (Haque, 2015). The graphics is plotted in STAR CCM+.

Figure 5.6 presents the pressure plot of the Hardangrbrua 2D plot. The simulations from this thesis are displayed as the black and red lines, where the black line is the top of the bridge grider and the red line is the bottom of the bridge girder. The black and red circles called "Experimental data" presents the results for the bridge analysed in "Shaping Effects on Aerodynamics of Long-Span Cable-Supported Bridge Deck by Unsteady RANS" by (Haque, 2015). As can be seen there are compliance between the experimental data and the data from bridge girder alternative 1. This means that the pressure applied in STAR CCM+ is dividing itself in the same way as the pressure applied in (Haque, 2015).

5.4. Lift and drag vs. angle of attack for bridge girder alternative 2

The angles of attack are compared to the data from «Isogeometric Modeling and Experimental Investigation of Moving-Domain Bridge Aerodynamics» (Helgedagsrud et al., 2019). The lift and drag analysis are only conducted on the second bridge girder alternative. This is because this is the most realistic and the one with the most comparable data. The data in Helgedagsrud et al. (2019) is from wind tunnel simulations so there might be some differences in the results. The simulation data is extracted from STAR CCM+ and the experimental data are the results from the wind tunnel. The graphics is presented from Excel. The bridge girder design for the experimental data is slightly different from the one in this thesis and this might have caused some differences in the results. These differences will be further discussed in the discussion. The bridge girder design is illustrated in Figure 5.7.

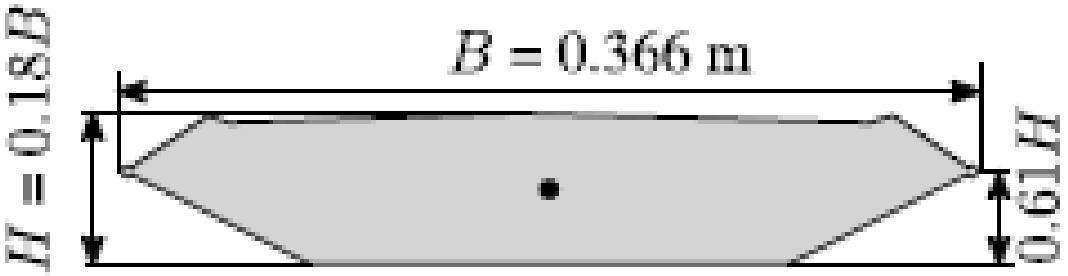

Figure 5.7: The bridge girder used as experimental data (Helgedagsrud et al., 2019).

The lift and drag are extracted from STAR CCM+ where the drag and lift are run for the analysis. The lift and drag coefficients are the calculated from the lift and drag forces.

5.4.1. Drag Coefficient (C_D)

The drag coefficient is extracted from the drag force plot in STAR CCM+ and calculated using Eq 2-1.

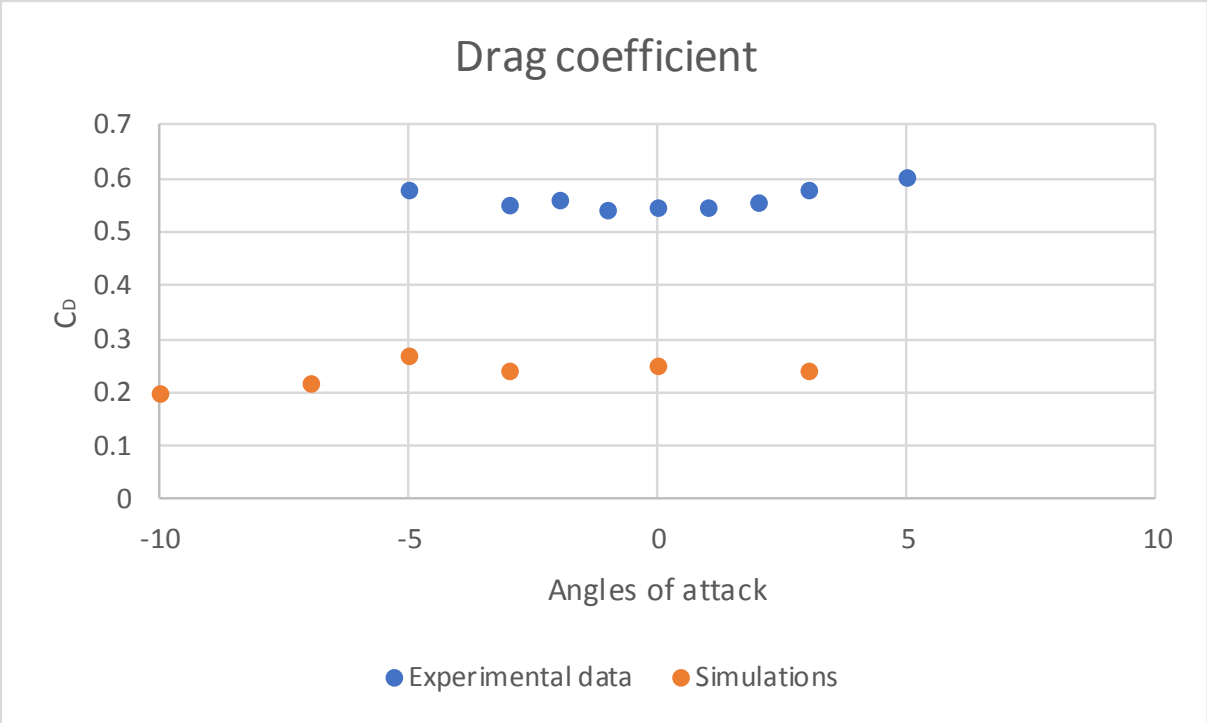

Figure 5.8: Drag Coefficient for different angles of attack extracted from STAR CCM+, calculated and converted in Excel.

Figure 5.8 presents the drag coefficient for the angles of attack from -10 to 3 degrees in relation to the experimental data from (Helgedagsrud et al., 2019). The simulated drag coefficients have lower values than the on for the experiment, but this is caused because of the differences in bridge girder geometry and that the simulations in this thesis is theoretical, while the once in the experiment is carried out in a wind tunnel simulation.

5.4.2. Lift Coefficient (C_L)

The lift coefficient is extracted from the lift force plot in STAR CCM+ and calculated using Eq 2-2.

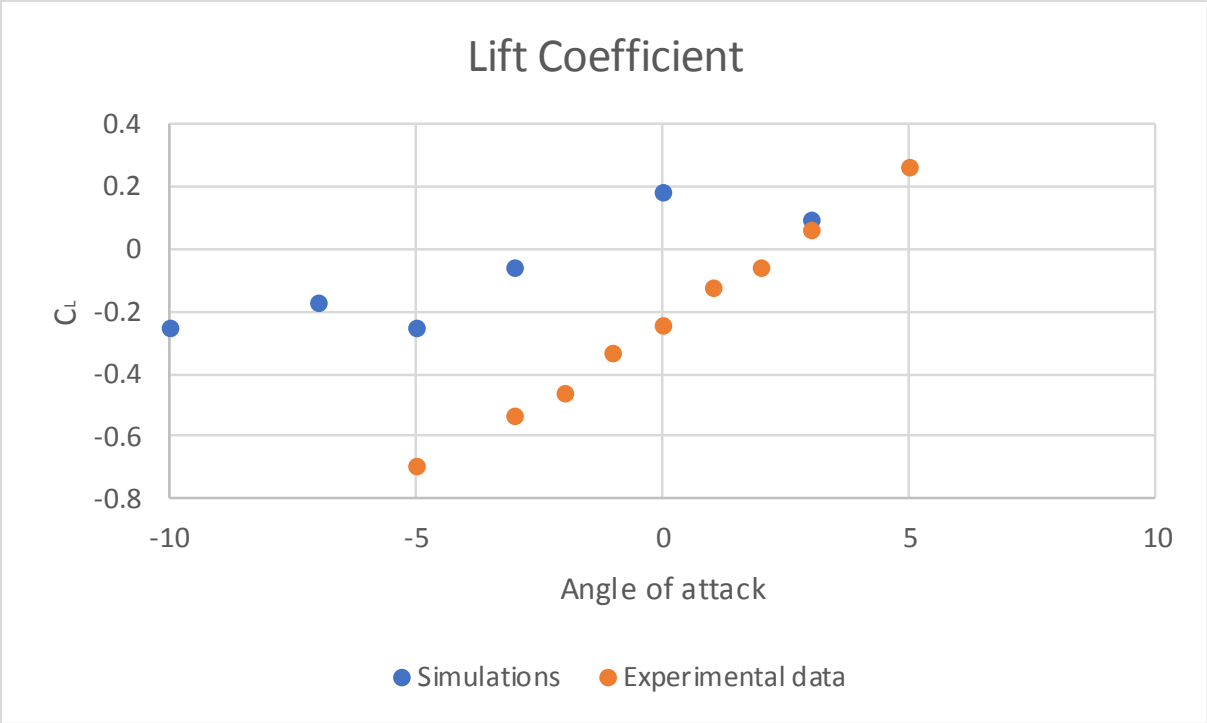

Figure 5.9: Lift Coefficient for different angles of attack extracted from STAR CCM+, calculated and converted in Excel.

Figure 5.9 presents the lift coefficient for the angles of attack from -10 to 3 degrees in relation to the experimental data from (Helgedagsrud et al., 2019). The simulated lift coefficients have higher values than the experimental data, but the slope is the same for the linear trend from 0 to -5 degrees. For 3, -7 and -10 degrees a separation has occurred, and the lift do not follow the linear trend.

6. Discussion

The discussion is derived into two parts. There will first be a general discussion around bridge girders and simulations, and then there will be the discussion on the simulations and analyses conducted in the previous chapters.

6.1. General discussion

The goal for this thesis was to conduct a validation study for a general bridge girder in comparison with other analyses of bridge girders in Norway and in the PhD thesis "Shaping Effects on Aerodynamics of Long-Span Cable-Supported Bridge Deck by Unsteady RANS" by (Haque, 2015). After conducting analyses there are ground for a discussion. In the PhD thesis there was used a Growth Factor (GF), this factor was used because the grid system in finite volume method (FVM) is very crucial to get accurate results. The grid should be expanded gently in regions of high gradients, to keep the truncation error small. Different Growth Factors was recommended and for instance Franke et al. (2011) and Tominaga et al. (2008) recommends a GF of 1.3. This is only one opinion on the Growth Factor size, and there are many examples on other sizes for the GF. In this thesis it is chosen not to look further into growth factors and the GF used in Haque (2015) is not further analysed.
Because all the results and analyses are normalized, and the experimental data is plotted from a pdf file and converted into STAR CCM+ there could be some deviation in the results and simulations. However, these results are chosen to be valid for this thesis.

Before the simulations in STAR CCM+ were run there were applied mesh to the model. The size of this mesh is crucial to the results for the simulations if the mesh is too rough the simulations could be less accurate. If the mesh is too fine the simulations and meshing will take a lot of time to run. So, the clue is to find a mesh that is a middle between these two criteria.
As for the mesh, the size of the computational domain is also crucial. If this domain is to small the simulations will be limited and not give accurate results. From the simulations run in this thesis it seems like the mesh and computational domain is in the right size and have not been affecting the results in a negative way.

6.2.Discussion on 2D simulations

When conducting the 2D simulations for the two bridge girders, the square and the rectangle, there were different factors that could have affected the results and simulations. There should be a good compliance between the simulations conducted in this thesis in relation to earlier work and analyses. The square, rectangle and the bridge girder alternative 1 has an inlet velocity of 3.0 m/s while the bridge girder alternative 2 and the different angles of attack has an inlet velocity in x-direction of 8.0 m/s and is scaled 50 times compared to bridge girder alternative 1. For the angles of attack the velocity varies, this is because the angles of attack are applied using different y-velocities. For instance, for 3 degrees angle of attack x-velocity is 8.0 m/s and y-velocity is 0.419 m/s, this gives an inlet velocity of 8.011 m/s. The reason for the change in velocity from 3.0 m/s to 8.0 m/s is that this is the velocity used in the journals that this thesis is seen in relation to.

The square and rectangle simulations were conducted to get insight in the simulations and there were a lot of previous work to compare it to. The square and rectangle simulations have a good compliance and coherence with previous work and the analysis conducted in this thesis are valid, since the PhD thesis found that previous research validated the papers findings. Since the simulations is only compared to data from one paper there could be some differences, but the compared data is undermined by previous work in the analysis, the validity of the paper should be good. In the 2D square simulations the data with GF 1.05 is chosen. The data in (Haque, 2015) had only small differences, and the data with the smallest GF was chosen. For both the square and the rectangle the pressure was highest on the inlet side (0-1 for the square, and 0-0.5 for the rectangle) this is because the inlet wind hits this side first. When hitting the square and the rectangle the wind velocity increases, and high pressure is applied to the geometry. The wind must move around the square and rectangle, and the pressure on the outlet side of the geometries is lower than the reference pressure.

To get better compliance in Figure 5.2 and Figure 5.4 there could have been run more iterations in STAR CCM+ to get more accurate results for the square and rectangle. Also, the sharp edges of the two geometries have a huge impact on the wind force and stream and will make it hard to have one specific wind phase for all simulations. If a new simulation had been run on the same geometry, there might have been a different wind pattern.

As can be seen in the bridge girder alternative 1 results (Figure 5.6) there are good compliance and coherence between the experimental data and the data conducted in this thesis. This also means that the simulations conducted in this thesis is valid in relation to (Haque, 2015). Had there been applied a different pressure or the pressure had been applied to different sides of the bridge girder, then there would be different results, and there might not have been any compliance between the two simulations. The same would be if the bridge girder geometry where not as similar as it is in this case. The small differences in the graphics could come from small differences in angles or side lengths for the two bridge girders. Both bridge girders analysed is bridges built today and are good bases for new bridge girders.

When it comes to the pressure simulations on the different angles of attack there are only small inequalities between them. After conducting simulations on all the different angles there can be seen some differences, but the angles are so small, so there are no big differences.

When the lift and drag coefficients are plotted the simulations for angles between 0 and -5 are valid and shows good compliance with previous work, while for degrees 3, -7 and -10 there are created separation in the flow. The separation leads to differences in the analyses compared to the rest of the angles, and the results are no longer linear.

7. Conclusion and further research

This chapter will conclude the previous work in this thesis then there will be sources of error that could have affected the thesis, and at last there will be some suggestions to further work and research to conduct around this theme.

7.1. Conclusion

After conducting the simulation and analysis it seems that the both bridge girders are valid in relation to previous work. Since there is not conducted analyses for different angles of attacks for the first alternative it is hard to say how it will react to this, but from the pressure analysis it is in good correlation to a similar bridge girder. For the second alternative the lift and drag analyses shows that the bridge girder has good results for 0 to -5 degrees angle of attack, while for 3, -7 and -10 degrees there is a separation in the simulation that leads to lack of lift of the bridge girder. In general, the analyses shows that the simulation conducted in this thesis is valid in relation to previous work.

7.2. Sources of error

There are different sources of error for this thesis. There could be some simulations errors or errors in the simulated models. Since the author did not have much knowledge about the aerodynamics or STAR CCM+ before starting the work on this thesis there could be errors due to the authors lack of knowledge. There are run different amount of iterations on the simulations, this could have made some of the simulations more accurate than others. The experimental data are received and simulated by others and the conditions around these simulations in unknown and therefor it is hard to know sources of error for these specific simulations. On the analysis for the bridge girder alternative 1 STAR CCM+ stops after 10 000 iterations in the analyses. Some of the results could have been more accurate with more iterations.

7.3.Further research

Based on experience gained during this thesis some recommendations for further research are suggested:

- Look at other geometries of bridge girders (different angles etc)
- Different inlet wind velocities
- Simulations on 3D models. Use the bridge girders from this model and test lift and drag forces in 3D to get more realistic results for research.

8. References

AIAA. (1998). Guide for the Verification and Validation of Computational Fluid Dynamics Simulations. *American Institute of Aeronautics and Astronomics*.

Bearman, P. & Obasaju, E. (1982). An experimental study of pressure fluctuations on fixed and oscillating square-section cylinders. *Journal of Fluid Mechanics*, 119: 297-321.

Bruno, L., Fransos, D., Coste, N. & Bosco, A. (2010). 3D flow around a rectangular cylinder: a computational study. *Journal of Wind Engineering and Industrial Aerodynamics*, 98 (6-7): 263-276.

Ferde. (2019). *Hardangerbrua*. Available at: https://ferde.no/om-oss/hardangerbrua/ (accessed: 13.02.2019).

Ferjefri E39. (2017). Statens Vegvesen Available at: https://www.vegvesen.no/vegprosjekter/ferjefriE39 (accessed: 31.1.2019).

Franke, J., Hellsten, A., Schlunzen, K. H. & Carissimo, B. (2011). The COST 732 Best Practice Guideline for CFD simulation of flows in the urban environment: a summary. *International Journal of Environment and Pollution*, 44 (1-4): 419-427.

Galli, F. (2005). Comportamento aerodinamico di strutture snelle non profilate: approccio sperimentale e computazionale. *MasterΓs thesis, Politecnico di Torino, Turin, Italy*.

Haque, M. (2015). Shaping effects on aerodynamics of long-span cable-supported bridge deck by Unsteady RANS.

Haque, M. N., Katsuchi, H., Yamada, H. & Nishio, M. (2013). Numerical simulation for effects of wind turbulence on flow field around rectangular cylinder. *構造工学論文集 A*, 59: 605-615.

Helgedagsrud, T. A., Bazilevs, Y., Korobenko, A., Mathisen, K. M. & Øiseth, O. A. (2018). Using ALE-VMS to compute aerodynamic derivatives of bridge sections. *Computers & Fluids*.

Helgedagsrud, T. A., Akkerman, I., Bazilevs, Y., Mathisen, K. M. & Øiseth, O. A. (2019). Isogeometric modeling and experimental investigation of moving-domain bridge aerodynamics. *Journal of Engineering Mechanics*, 145 (5): 04019026.

Jayakumar, J., Mahajani, S., Mandal, J., Iyer, K. N. & Vijayan, P. (2010). CFD analysis of single-phase flows inside helically coiled tubes. *Computers & chemical engineering*, 34 (4): 430-446.

Kenis, P. J., Ismagilov, R. F. & Whitesides, G. M. (1999). Microfabrication inside capillaries using multiphase laminar flow patterning. *Science*, 285 (5424): 83-85.

Lee, B. (1975). The effect of turbulence on the surface pressure field of a square prism. *Journal of Fluid Mechanics*, 69 (2): 263-282.

Mannini, C., Šoda, A. & Schewe, G. (2010). Unsteady RANS modelling of flow past a rectangular cylinder: Investigation of Reynolds number effects. *Computers & fluids*, 39 (9): 1609-1624.

Matsumoto, M., Shirato, H., Araki, K., Haramura, T. & Hashimoto, T. (2003). Spanwise coherence characteristics of surface pressure field on 2-D bluff bodies. *Journal of Wind Engineering and Industrial Aerodynamics*, 91 (1-2): 155-163.

Mema, I., Mahajan, V. V., Fitzgerald, B. W. & Padding, J. T. (2019). Effect of lift force and hydrodynamic torque on fluidisation of non-spherical particles. *Chemical Engineering Science*, 195: 642-656.

Menter, F. R. (1992). Improved two-equation k-omega turbulence models for aerodynamic flows.

Montgomery, R. (1947). Viscosity and thermal conductivity of air and diffusivity of water vapor in air. *Journal of Meteorology*, 4 (6): 193-196.

Ohtsuki, Y. (1978). *Wind tunnel experiments on aerodynamic forces and pressure distributions of rectangular cylinders in a uniform flow*. Proc. 5th Symp. on Wind effects on structures.

Pope, S. B. & Pope, S. B. (2000). *Turbulent flows*: Cambridge university press.

Ricciardelli, F. & Marra, A. M. (2008). *Sectional aerodynamic forces and their longitudinal correlation on a vibrating 5: 1 rectangular cylinder*. Proceedings of the 6th International Colloquium on Bluff Body Aerodynamics and Applications, Milan, Italy.

Science. (2013). Russian Culture archive. Available at: http://russiaprofile.org/photos/52678_7.htmlx (accessed: 13.05.2019).

Siemens. (2018). *STAR-CCM+ tutorial*.

Sjødin, B. (2016). *What's The Difference Between FEM, FDM, and FVM?*: COMSOL. Available at: https://www.machinedesign.com/fea-and-simulation/what-s-difference-between-fem-fdm-and-fvm (accessed: 12.02.2019).

Strømmen, E. (2010). *Theory of bridge aerodynamics*: Springer Science & Business Media.

Tang, H., Shum, K. & Li, Y. (2019). Investigation of flutter performance of a twin-box bridge girder at large angles of attack. *Journal of Wind Engineering and Industrial Aerodynamics*, 186: 192-203.

Tipler, P. A. & Mosca, G. (2007). *Physics for scientists and engineers*: Macmillan.

Tominaga, Y., Mochida, A., Yoshie, R., Kataoka, H., Nozu, T., Yoshikawa, M. & Shirasawa, T. (2008). AIJ guidelines for practical applications of CFD to pedestrian wind environment around buildings. *Journal of wind engineering and industrial aerodynamics*, 96 (10-11): 1749-1761.

Weisstein, E. W. (2007). *Bernoulli's Law*. Wolfram Research Available at: http://scienceworld.wolfram.com/physics/BernoullisLaw.html (accessed: 13.05.2019).

Wong, K. L. & Chen, C. o. K. (1986). Finite element solutions for laminar flow and heat transfer around a square prism. *Journal of the Chinese institute of Engineers*, 9 (6): 605-615.

Yang, Y., Zhou, R., Ge, Y. & Zhang, L. (2016). Experimental studies on VIV performance and countermeasures for twin-box girder bridges with various slot width ratios. *Journal of Fluids and Structures*, 66: 476-489. doi: https://doi.org/10.1016/j.jfluidstructs.2016.08.010.

Öktem, H., Erzurumlu, T. & Kurtaran, H. (2005). Application of response surface methodology in the optimization of cutting conditions for surface roughness. *Journal of materials processing technology*, 170 (1-2): 11-16.

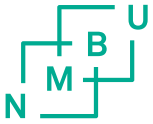

Norges miljø- og biovitenskapelige universitet
Noregs miljø- og biovitskapelege universitet
Norwegian University of Life Sciences

Postboks 5003
NO-1432 Ås
Norway